Correlations of the Rosebery-Hercules Host Sequence at White Spur, Mt Read Volcanics, western Tasmania: Implications for Exploration

Corey Malcolm Jago

BSc.

UNIVERSITY OF TASMANIA

School of Earth Sciences

CODES

ARC Centre of Excellence in Ore Deposits

A research thesis submitted in partial fulfilment of the requirements for an Honours degree at the School of Earth Sciences, University of Tasmania.

November 2005

Declaration

This thesis contains no material which has been accepted for the award of any other degree or diploma in any tertiary institution, and to the best of my knowledge and belief, contains no material previously published or written by another person, except where due reference is made in the text of the thesis.

Signed

Corey Jago BSc.

Abstract

The contact between the Central Volcanic Complex (CVC) and the White Spur Formation at White Spur is considered prospective for VHMS ore deposits similar to those at Rosebery and Hercules. The contact and the major lithostratigraphic units above and below the contact were examined through detailed drillcore logging and mapping of selected areas.

The CVC at White Spur includes extensive feldspar-phyric pumice breccia that grades to stratified, pumiceous, crystal-rich sandstone and siltstone known as the Host Rock. The CVC also includes feldspar-phyric dacite originally emplaced as a dome or shallow intrusion. The White Spur Formation consists of six main units including laminated pyritic black mudstone, quartz-feldspar-biotite-phyric rhyolite, three quartz-feldspar-phyric volcaniclastic units (a rhyolitic pumice-lithic breccia mass-flow unit, a massive sulfide clast-bearing mass-flow unit, and a crystal-rich mass-flow unit) and an interbedded mudstone and sandstone turbidite unit. Composition, lithology, textures, internal organisation and spatial relationships were used to differentiate among the three quartz-feldspar-phyric mass-flow units. All the major units were deposited in a relatively deep submarine setting. Although some parts of the stratigraphy were removed locally by erosion and/or faults, there is no evidence of subaerial environments.

Correlations of the main units in the CVC and White Spur Formation were assessed by means of fence diagrams. Sub-basins identified in the CVC probably developed in response to syn-depositional faults. The Host Rock was preferentially preserved in these sub-basins. The three volcaniclastic mass-flow units of the White Spur Formation were deposited on top of the CVC and can be correlated across much of the area. The middle volcaniclastic mass-flow unit (the massive sulphide clast-bearing mass-flow unit) is particularly important because it records the presence of a coeval massive sulphide deposit at a location up-current of present exposures. The White Spur area includes several targets for exploration: locations where the Host Rock is present, sites of known significant mineralisation, and places where structural controls, such as syn-depositional growth faults have been identified. Exploration focusing on the Host Rock along strike and down-dip in known occurrences at White Spur could lead to further VHMS discoveries.

Acknowledgments

This year has certainly been the most eventful year of my life. All of my hard work and dedication has culminated into this thesis. I need to thank many people for assistance and support throughout the year.

I need to begin by thanking my supervisors Prof. Jocelyn McPhie, Andrew McNeill and Wally Herrmann for their guidance and assistance throughout the year. Thank you Jocelyn for all your time spent assisting me, especially in this last week. I would like to thank Andrew for all his guidance with this project during the year and particularly with the fieldwork, notably his shortcuts… Appreciation is given to Wally for all his support on all matters of the honours year, he always knows what to say.

I like to thank Craig Archer for all his help during fieldwork and the 'discussions' we had, there were a few. I would like to thank Trent Wheldon for his unconditional help during the fieldwork. Mick Skikra is thanked for his indescribable aid during core logging.

I cannot overlook the 2005 Geology Honours Crew for what they have done this year. It has been a great year and thanks go to Joel, John, Brendan, Mel, Kat, Adam, Sam and especially Kim. Thankyou for everything and I wish you all the best for the future!

To all my great friends who I have met over the past four years, I thankyou dearly and appreciate all of you for your overwhelming friendship and support over the years.

Last but not least, I would like to thank my family for the constant love and support throughout the year.

Thankyou everyone.

Table of Contents

List of Tables and Figures

Figures

Tables

Plates

List of Appendices

Chapter 1 Introduction

1.1 Exploration and Scientific Interest

The lateral extensions of the Rosebery-Hercules host unit have been an important focus of regional exploration in the Mt Read Volcanics from Bastyan Dam to the Hall Rivulet Canal area in western Tasmania. Identification of the host interval includes recognition of a major lithological change from very thick units of feldspar-phyric rhyolitic and dacitic and mainly volcaniclastic rocks (Central Volcanic Complex) to a more varied succession of quartz + feldspar-phyric rhyolitic, volcaniclastic rocks, feldspar ± hornblende-phyric or pyroxene-phyric andesite and basalt, and mudstone (White Spur Formation). This change marks an internal stratigraphic boundary in the northern Mt Read Volcanics that coincides with the Rosebery and Hercules massive sulfide ore lenses. The change in facies and the formation of the mineralising hydrothermal systems could both reflect regional tectonic events.

The host interval location and the contact between the White Spur Formation and Central Volcanic Complex (CVC) from Rosebery and Hercules are well established. These are poorly known in the White Spur area. Hence, the aims of this project are to:

1. Define the position of the internal stratigraphic boundary between the CVC and White Spur Formation from South Hercules to Hall Rivulet Canal, using existing maps, detailed core logging and surface mapping of selected areas.

2. Establish the textural and compositional characteristics of the volcanic and sedimentary facies at the top of the CVC immediately below the host interval, and of the overlying units (White Spur Formation or equivalent).

3. Describe the lateral and vertical variations in the facies adjacent to the boundary and represent the changes on long-sections and cross-sections.

The results will refine current understanding of the internal and correlations, the position of the ore horizon in relation to volcanic and sedimentary units, and the timing of volcanic, and mineralising events during evolution of the central part of the Mt Read Volcanics. Characterisation and location of the CVC and White Spur Formation stratigraphic

boundary will also have implications for exploration in the Mt Read Volcanics, as the boundary is considered highly prospective.

1.2 Study methods

This study investigated the White Spur Formation and CVC contact by detailed outcrop mapping and examination of cores from five diamond drill holes. Core logging was completed at the Zinifex core yard in Tullah for 5 weeks, travelling from Rosebery daily. Drillcore was logged at 1:200 scale but one of the contact intercepts was logged at a more detailed scale (1:20). Selected areas around White Spur were mapped in 3 days. Maps and logged stratigraphic sections of the outcrops were produced.

The project involved volcanic facies analysis. Compositional and textural data form the basis for differentiating among the volcanic and sedimentary facies and defining stratigraphic units (chapter 4) and correlation work (chapter 5). Correlation of the stratigraphic units was undertaken by constructing and updating litho-stratigraphic 'fence diagrams' integrated with previous work by Allen (1997 unpub.). Facies descriptions were assisted by examining numerous thin sections from each of the major facies.

There was no attempt to describe and delineate alteration facies in the area. Altered zones occur in drillcore and outcrop (noted in logging) and used to assist in description and stratigraphic correlations only.

1.3 Study Area

White Spur is located in western Tasmania close to the townships of Rosebery, Zeehan and Queenstown and is about 10.5 km south of Rosebery (Figure 1.1). The White Spur EL 5/96 contains an area of 19 km^2 on the southwestern flanks of Mt Read. The EL was obtained for exploration of potential volcanic hosted massive sulfide (VHMS) deposits. It was formerly held by Renison Limited and explored by RGC exploration but is now held by Zinifex Limited. The study area extends over 6 km from South Hercules to the Anneliese prospect, concentrating on the area between South Hercules and the WSP 10/10A drillhole (Figure 1.1).

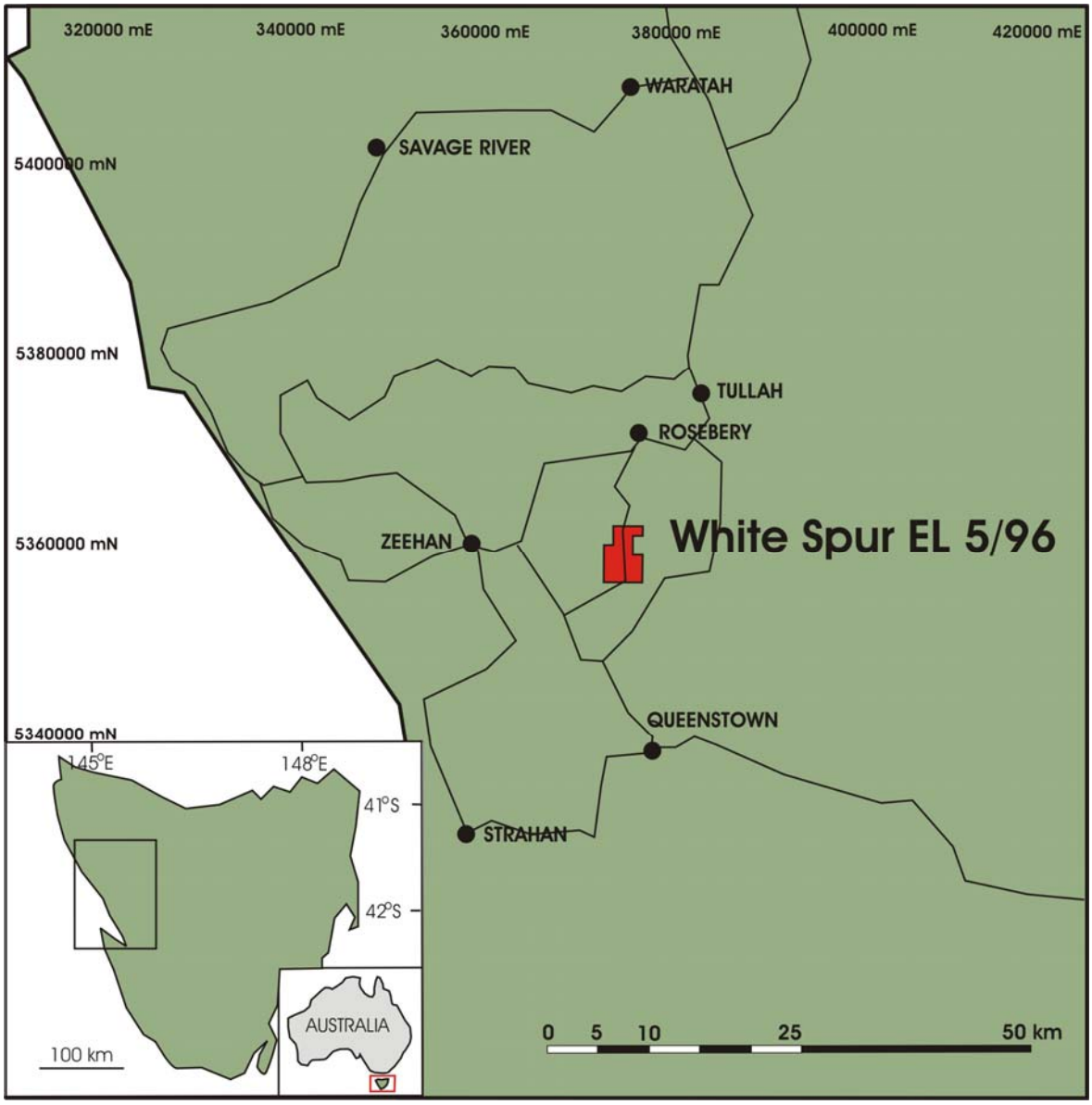

Figure 1.1: Locality map of western Tasmania showing the White Spur EL 5/96 (Modified from Vicary, 1998).

The northern part of Howards Road allows access to the White Spur area from the Anthony Road. A HEC road that follows the Hall Rivulet Canal provides access within the area. 4WD vehicles can reach more remote areas via old logging tracks. The Hercules Haulage road and Howards Track, which pass through the Hercules and South Hercules area and the northern end of the White Spur EL, are accessible via the derelict Williamsford township.

The topography is rugged, as is typical of western Tasmania. The ridge crests have alpine

heath and shrubs whereas the slopes and valleys contain dense rainforest Myrtle and King Billy Pine vegetation that presents difficulties for detailed geological mapping.

1.4 Previous Work

The Mt Read Volcanics have been studied extensively due to the economic importance. Regional studies have been undertaken by numerous authors. Corbett (1981, 1992) studied the stratigraphy of the Mt Read Volcanics with an emphasis on the volcanic setting of the massive sulfide ore bodies. Corbett (2002) compiled work from numerous authors and updated stratigraphic interpretations of the Mt Read Volcanics. McPhie and Allen (1992) described the facies architecture on a regional scale from Hellyer to White Spur whereas Gifkins (2001) documented the volcanic facies and alteration in the northern CVC.

Crawford et al. (1992) drew important tectonic implications from the composition of igneous units in the Mt Read Volcanics. Contemporaneously, Crawford and Berry (1992) proposed a tectonic model for the formation of the Mt Read Volcanics.

The White Spur Formation was first described by Corbett and Lees (1987). Since then, almost all major studies of the stratigraphy, structure and mineralisation of the formation have been unpublished (Allen, 1991 unpub.; 1997 unpub.; 1998 unpub.; Dugdale, 1992; Nunn, 1995; Vicary, 1998).

The Rosebery and Hercules massive sulfide deposits have been comprehensively researched. Brathwaite (1969, 1972) described their geological setting and proposed an origin for the Rosebery deposit. Green et al. (1981) discussed the geology and composition of the Rosebery ore deposit. Lees (1987 unpub.) studied the Rosebery and Hercules ore deposits and compiled all the known data on the Hercules deposit, as no formal comprehensive publication existed at that stage. Zaw and Large (1992) described the mineralisation and associated alteration assemblages of the South Hercules deposit in detail.

1.5 Thesis Outline

Chapter 1 includes introductory information. Chapter 2 provides a discussion of the regional geology of the Mt Read Volcanics with attention on the major lithostratigraphic

and VHMS deposits. Chapter 3 includes an examination of the White Spur geology, in particular the main geological units and the structure of the area. Chapter 4 deals in detail with the main volcano-sedimentary facies and facies associations of White Spur and the stratigraphic positioning of these lithofacies. Chapter 5 considers the correlations of the major stratigraphic units in the White Spur area and presents an interpretation of the facies architecture of the area. Chapter 6 summaries the exploration potential and mineralisation at White Spur, using the new stratigraphic framework developed. Chapter 7 provides a summary of principal conclusions presented in the thesis.

Chapter 2 The Regional Geology of the Mt Read Volcanics

2.1 Introduction

This chapter summarises the regional lithostratigraphy, tectonic and palaeo-environmental setting, and subsequent deformation of the Mt Read Volcanics.

The Mt Read Volcanics occupy a 200 km long and 20 km wide belt and consist of Middle to Late Cambrian volcanic and non-volcanic sedimentary rocks (Corbett, 1992; Crawford et al., 1992; Gifkins, 2001; McPhie and Allen, 1992). The belt extends from Elliott Bay to Deloraine in an arcuate against the western and northern margin of the Precambrian Tyennan Region (Crawford and Berry, 1992; Crawford et al., 1992; Gifkins, 2001).

2.2 Volcanic facies associations, tectonic setting, and deformation

Compositionally and texturally diverse lavas, syn-volcanic intrusions and syn-eruptive volcaniclastic units are the predominant volcanic facies associations of the Mt Read Volcanics (Gifkins et al., 2005a; McPhie and Allen, 1992). All facies were emplaced in an submarine environment below wave base (McPhie and Allen, 1992). The lavas and intrusions have calc-alkaline, primarily felsic compositions (Crawford et al., 1992; Gifkins, 2001). Thick and extensive, rhyolitic or dacitic, pumice-rich and crystal-rich units and in situ and resedimented hyaloclastite are typical of the volcaniclastic facies associations (McPhie and Allen, 1992). Sedimentary facies including black mudstone and graded, bedded sandstone derived from volcanic and Precambrian metasedimentary basement sources are interbedded with the volcanic facies (McPhie and Allen, 1992).

The Mt Read Volcanics were formed in a post–collisional tectonic setting, which followed a mid-Middle Cambrian 510 Ma arc–continent collision (Crawford and Berry, 1992; Munker and Crawford, 2000).

Deformation of the belt in the Late Cambrian involved syn-depositional faults such as the Rosebery Fault and Henty Fault Zone (Crawford & Berry, 1992). The Henty Fault

divides into north and south components that form the boundaries of the poorly understood Henty Fault Wedge. The Devonian Tabberabberan Orogeny was responsible for N-S trending folds in the Mt Read Volcanics, regional metamorphism, the reactivation of older Cambrian faults (Rosebery Fault. Mt Black Fault, Henty Fault) as reverse faults and the production of two cleavages throughout the volcanic belt (Berry, 1989).

The worldwide known Mt Read Volcanics are highly mineralised. The succession contains six large VHMS-type deposits including Hellyer, Que River, Rosebery, Hercules, Henty and Mt Lyell and a number of VHMS style prospects (Figure 2.1).

2.3 Major lithostratigraphic units

The distinctive lithostratigraphic units of the Mt Read Volcanics include the Sticht Range Beds, Eastern quartz-phyric sequence, the CVC, the Western volcano-sedimentary sequence and the Tyndall Group.

2.3.1 Sticht Range Beds

The Sticht Range Beds are interbedded sedimentary and volcaniclastic rocks, which exist in a thin basal unit of at the eastern side of the Mt Read Volcanics, overlying the Precambrian Tyennan basement (Corbett, 1992; Gifkins, 2001). The beds comprise siliciclastic pebble-cobble conglomerate, sandstone, interbedded micaceous siltstone with minor interbedded volcaniclastic units that dip and face west (Corbett, 1992). The beds mainly contain Precambrian detritus and varying volcanic detritus (Corbett, 1992; Gifkins, 2001).

The contact between the Sticht Range Beds and the Precambrian basement is an angular unconformity locally faulted (Corbett, 1992). Upward fining in the sequence suggests a depositional progression from fluvial to shallow marine and deeper marine environments (Corbett, 1992; Gifkins, 2001). Poorly preserved probable Middle Cambrian aged trilobites exist near top of the sequence at Lake Dora (Corbett, 1992).

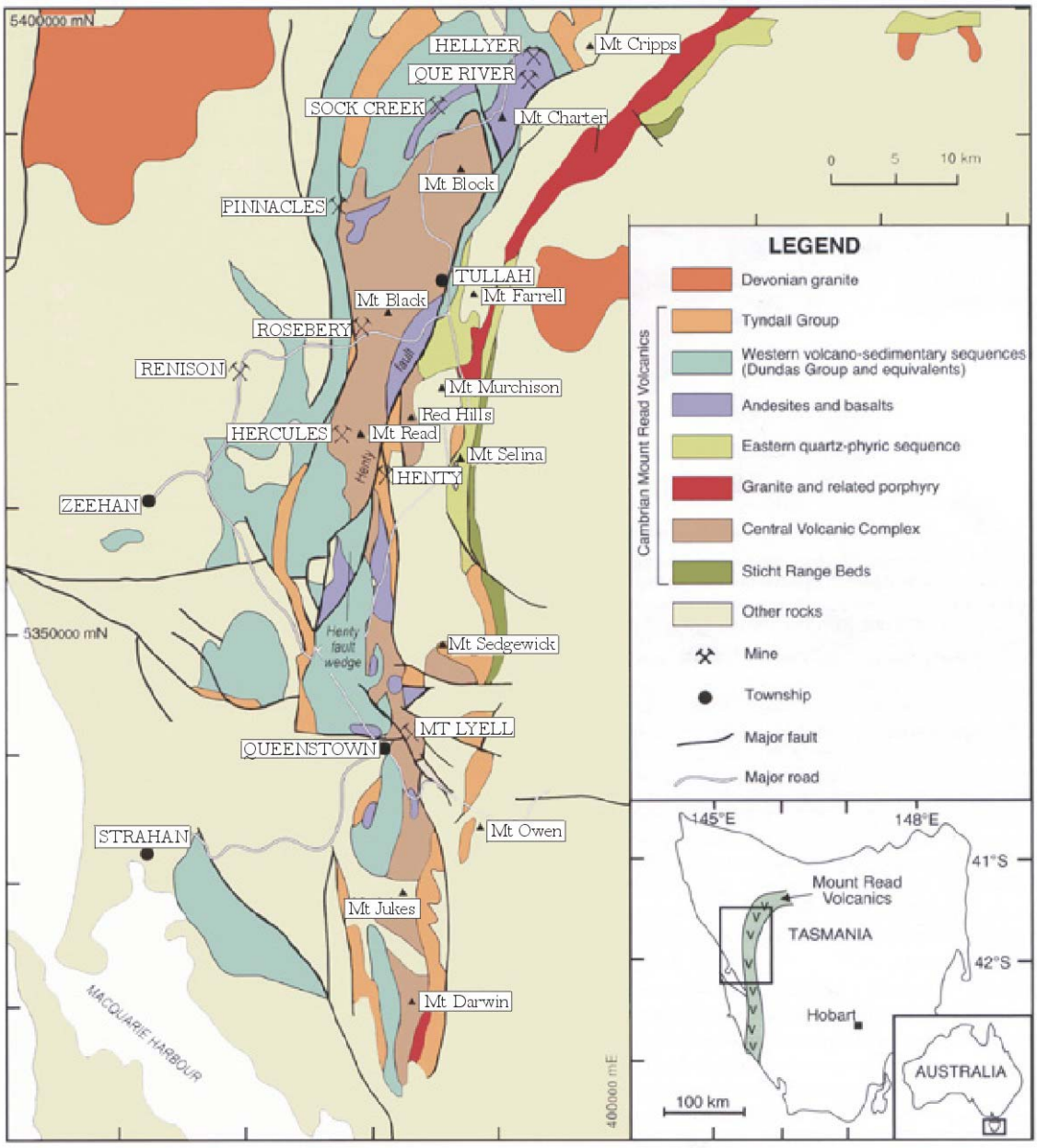

Figure 2.1: Geological map of the main lithostratigraphic units and major massive sulfide deposits of the Mt Read Volcanics, western Tasmania (Modified from Gifkins et al., 2005a).

2.3.2 Eastern quartz-phyric sequence

The Eastern quartz-phyric sequence is restricted to the eastern side of the Mt Read Volcanics (Gifkins, 2001). It overlies the Sticht Range Beds at Lake Dora and Mt Farrell, interfingers with the CVC, and is overlain conformably by the Western volcano-sedimentary sequence (Corbett, 1992; Gifkins, 2001).

The sequence mainly includes felsic, quartz-feldspar-phyric lavas, volcaniclastic rocks, abundant syn-volcanic quartz-feldspar (± biotite) porphyry intrusions and minor related granitoids (Corbett, 1992; Gifkins, 2001). The succession overlies the Precambrian continental basement (Crawford et al., 1992).

A conformable contact between the Eastern quartz-phyric sequence and the west dipping and facing, younger Farrell Slates occurs at the western end of the Murchison Gorge (Corbett, 1992). Slate and tuffaceous sandstone occur in the Farrell Slate sequence (Corbett, 1992).

Corbett (1992) interpreted a subaqueous setting for the eastern quartz-phyric sequence based on the numerous units of bedded sandstone, siltstone and shard-rich mudstone, some with common Precambrian-derived detritus.

2.3.3 Central Volcanic Complex

The central part of the Mt Read Volcanics is a predominantly feldspar-phyric, felsic volcanic sequence that extends from South Darwin Peak to Mt Murchison on the southern side of the Henty Fault (southern CVC) and from Mt Read to Mt Block on the northern side (northern CVC) (Corbett, 1992; Crawford et al., 1992; Gifkins, 2001).

Feldspar-phyric rhyolitic-dacitic lavas, pumciceous volcaniclastic units and syn-volcanic intrusions dominate the CVC and are locally intercalated andesites and basalts (Corbett, 1992; Crawford et al., 1992; Gifkins, 2001 unpub.). The feldspar-phyric lavas and syn-volcanic intrusions are typically massive and have common flow-banding and autobrecciation textures, also some dome-like bodies contain columnar jointing (Corbett, 1992; Crawford et al., 1992; Gifkins, 2001). Albite phenocrysts are common in the lavas. Small sparse quartz phenocrysts are rare in the commonly spherulitic groundmass (Corbett, 1992).

The northern CVC contains quartz-feldspar-phyric intrusions and tholeiitic basalt and dolerite dykes (Henty Dyke Swarm). The northern CVC lacks Cambrian granites and associated K-altered rocks potash-rich rocks (6-9% K_20) that are characteristic of the southern CVC (Corbett, 1992; Crawford et al., 1992; Gifkins, 2001). The Rosebery and Hercules host sequence is an east-dipping volcaniclastic-rich sequence at the western

margin of the northern CVC (Corbett, 1992). Units within the sequence include the Footwall Volcaniclastics, Host Rocks, Black Slate and Hangingwall Volcaniclastics (Corbett, 1992).

The Dundas and Mt Charter Groups of the Western volcano-sedimentary sequence conformably and disconformably overlie and also interfinger with the northern CVC (Gifkins, 2001). The Yolande River sequence of the Western volcano-sedimentary sequence lies to the west of the southern CVC (Gifkins, 2001). To the east, interfingering relationships with the Eastern quartz-phyric sequence and the southern CVC are present and these two units are considered to be coeval (Crawford et al., 1992; Gifkins, 2001). The Tyndall Group and Anthony Road Andesite overlie the southern CVC to the east.

The CVC hosts many of the major VHMS and Au deposits including Rosebery, Hercules and Mt Lyell, and several other prospects. Rosebery and Hercules occur in an east-facing volcaniclastic-rich sequence with an overlying thick felsic lava sequence at the western margin of the northern CVC (Corbett, 1992). The Mt Lyell deposits, in contrast, appear to lie near the stratigraphic top of the CVC, just below the Tyndall Group, at the eastern margin of the southern CVC.

The CVC was originally thought to have been subaerial due to the abundance of lavas and pumice-rich 'ignimbrites' and rare bedded sedimentary rocks (Corbett, 1992). Studies now suggest that the extensive pumiceous units are submarine mass-flow deposits of unwelded pumice where compaction and metamorphism created false welded textures (Corbett, 1992). Other evidence such as hyaloclastite and turbidites indicates a subaqueous depositional environment (Corbett, 1992). Therefore, a subaqueous setting for most of, or all of the CVC is accepted (Corbett, 1992).

2.3.4 Western volcano-sedimentary sequence

This extensive marine volcano-sedimentary sequence extends from Mt Darwin to Mt Block along the western margin of the Mt Read Volcanics (Corbett, 1992). It contains interbedded quartz-feldspar-phyric tuffaceous mass-flow breccia units, turbidites sandstone, shard-rich tuffaceous mudstone, micaceous siltstone, and black graphitic shale intercalated with minor rhyolitic and andesitic lavas and large syn-volcanic porphyry

intrusions (Corbett, 1992; Gifkins, 2001).

The Western volcano-sedimentary sequence interfingers with the CVC in the central Mt Read Volcanics (Gifkins, 2001; McPhie and Allen, 1992), and overlies the Success Creek Group and the Crimson Creek Formation to the west (Gifkins, 2001).

A below wave base submarine setting is suggested from pillow basalts, hyaloclastite, pyritic mudstone, laminated fossiliferous mudstone, turbidites, mass-flow units and massive sulfide deposits being present in the sequence (Gifkins, 2001; McPhie and Allen, 1992).

The Western volcano-sedimentary sequence is sub-divided into 4 main units (Corbett, 1992; Crawford et al., 1992; Dugdale, 1992; Gifkins, 2001; McPhie and Allen, 1992; Nunn, 1995);

- the Yolande River sequence south of the South Henty Fault,
- the Dundas Group north of the North Henty Fault to the Pinnacles area,
- the Mt Charter Group near Hellyer; and
- the Henty fault wedge sequence.

The Yolande River sequence generally dips and youngs west, except in its easternmost part where a major anticline produced easterly dip and facing directions (Corbett, 1992). The tholeiitic Miners Ridge basalt lies near the base of the sequence. A siliciclastic sandstone unit called the Miners Ridge Sandstone exposed in the anticlinal core at Miners Ridge is the oldest part of the sequence (Corbett, 1992; Crawford et al., 1992). Near Lynchford, the Lynch Creek basalts include andesitic-basaltic rocks and similar rocks occur in the Howards Plains area (Corbett, 1992; Crawford et al., 1992). North and south of Queenstown, the Yolande River sequence was intruded by large quartz-feldspar ± biotite porphyry intrusions associated with lavas and pyroclastic rocks (Corbett, 1992; Crawford et al., 1992).

The Dundas Group extends from Dundas to Hercules and Rosebery to the Pinnacles area (Crawford et al., 1992). At Dundas, the sequence contact (the White Spur Formation) is

faulted against ultramafic-mafic complexes with the overlying conglomerates containing ultramafic detritus (Corbett, 1992; Crawford et al., 1992).

The White Spur Formation occurs at the base of the Dundas Group west of Hercules and unconformity overlies the CVC (Corbett, 1992; Corbett and Lees, 1987; Crawford et al., 1992). The White Spur Formation is a thick, west younging direction of feldspar-quartz-phyric, crystal-rich and pumice-rich volcaniclastic mass-flow deposits interbedded with lithic sandstone, siltstone, and shale (Corbett, 1992; Gifkins, 2001). Fossils found in the White Spur Formation date the Dundas Group at early Late Cambrian age while in the Dundas area, a Middle Cambrian age is acquired (Corbett, 1992).

The Dundas Group extends into the Rosebery-Pinnacles area as fault-disrupted sequences and into the Huskisson River area northeast of Renison where they are termed the Huskisson Group (Corbett, 1992). Volcanogenic detritus from the Mt Read Volcanics is common in the Middle Cambrian units of the lower Huskisson Group, but absent in the Late Cambrian units of the upper Huskisson and Dundas Groups (Corbett, 1992). The upper Dundas Group is likely an offshore equivalent of the Owen Conglomerate (Corbett, 1992).

The Mt Charter Group is a volcano-sedimentary sequence that occurs in the Sock Creek-Mt Charter-Mt Cripps area and contains 7 separate components (Corbett, 1992). The base of the Mt Charter Group contains the Que-Hellyer Volcanics composed of calc-alkaline andesitic-basaltic lavas and volcaniclastic units that host Hellyer and Que River VHMS deposits (Corbett, 1992; Gifkins, 2001). An interfingering relationship with the CVC and the lower sequence exists (Crawford et al., 1992).

The Southwell Subgroup is the uppermost unit of the Mt Charter Group (Corbett, 1992; Gifkins, 2001; McPhie and Allen, 1992). This unit contains quartz-phyric mass-flow units interbedded with black mudstone and Precambrian-derived turbidites that are similar lithologically to the White Spur Formation and the Rosebery-Hercules Hangingwall volcaniclastics (Corbett, 1992; Gifkins, 2001; McPhie and Allen, 1992). The Mt Cripps Subgroup units in the Mt Cripps-Two Hummocks area is a correlate of the Tyndall Group and resembles the Tyndall Group at Queenstown (Corbett, 1992).

2.3.5 Tyndall Group

The Tyndall Group is the youngest lithostratigraphic unit of the Mt Read Volcanics and is a dominantly submarine, volcano-sedimentary succession (Gifkins, 2001; White and McPhie, 1996; White and McPhie, 1997). The unit occurs as a narrow discontinuous belt that extends along the eastern margin of the Mt Read Volcanics (Gifkins, 2001; White and McPhie, 1997).

The Tyndall Group unconformably overlies the Tyennan basement and all major units of the Mt Read Volcanics including the Sticht Range beds, southern CVC, Eastern quartz-phyric sequence, Western volcano-sedimentary sequence, and the Cambrian Darwin granite (Gifkins, 2001; White and McPhie, 1997). The Owen Conglomerate conformably and unconformably overlies the Tyndall Group (Gifkins, 2001; White and McPhie, 1997). Correlates of the Tyndall Group occur in the upper Mt Charter Group near the Cradle Mountain Link Road and in the Winterbrook area, and within the Western volcano-sedimentary sequence in the Pinnacles area (White and McPhie, 1996). The thickness varies near Mt Lyell from 100-200 m to 1300 m in the Cradle Mountain Link Road area (White and McPhie, 1997). The Henty Au deposit is hosted near the base of the Tyndall Group along with several massive sulfide prospects (Gifkins, 2001).

The presence of late Middle Cambrian to early Late Cambrian fossils and regional stratigraphic relationships suggest the young age of the group (White and McPhie, 1997). An age of 494.4 ± 3.8 Ma for the Tyndall Group was determined by isotopic U-Pb dating of magmatic zircons and an age of 502.4 ± 3.5 Ma for the other Mt Read Volcanics units was acquired (White and McPhie, 1997).

The Tyndall Group is subdivided based on different provenance characteristics suggested from regional compositional variations and lithology (Gifkins, 2001; White and McPhie, 1996). The group is divided into the lower Comstock Formation and the upper Zig Zag Hill Formation (White and McPhie, 1996). Rhyolitic to dacitic juvenile volcanic components are characteristic of the Comstock Formation, whereas conglomerates of volcanic, mixed volcanic and basement provenance are typical of the Zig Zag Hill Formation (Gifkins, 2001). Further subdivision of the Comstock Formation into the Lynchford Member and the overlying Mt Julia Member is applicable (White and McPhie,

1996).

The volcanic lithofacies of both formations were probably deposited from high to low-density currents imply a subaqueous depositional setting below storm wave base (White and McPhie, 1997). The group is interpreted to have been deposited in much shallower waters than the preceding Mt Read Volcanics (McPhie and Allen, 2003; White and McPhie, 1996). Evidence includes a shallow marine fossil assemblage within limestone near the base of the group and also the volcaniclastic units contain common well-rounded clasts (McPhie and Allen, 2003; White and McPhie, 1996). Subaerial or shallow-marine explosive volcanic eruptions produced pyroclastic flows that created the crystal-rich volcaniclastic facies of the Comstock Formation after moving into the sea and transforming into water-supported mass-flows (White and McPhie, 1996).

The volcaniclastic facies of the Comstock Formation are syn-eruptive and the Zig Zag Hill Formation is dominated by epiclastic debris formed by post-eruptive erosion and reworking of the subaerial to shallow-marine source areas (White and McPhie, 1996).

2.4 Major VHMS deposits of the northern CVC

2.4.1 Rosebery VHMS deposit

The world – class Rosebery base metal deposit is one of the largest massive sulfide ore deposits in the Mt Read Volcanics of western Tasmania (Table 2.1). The polymetallic deposit comprises at least 16 tabular lenses that vary from 0.1 – 5 Mt in size (Green et al., 1981; Large et al., 2001; Solomon et al., 2004). The lenses are hosted in a felsic volcanic and sedimentary sequence that dips 45^{o} E over a strike length of over 2000 m to at least a 800 m depth (Green et al., 1981; Large et al., 2001; Solomon et al., 2004).

The lenses comprise massive and banded sphalerite, galena, pyrite, chalcopyrite and barite (Gifkins et al., 2005a). Minor minerals include tetrahedrite-tennantite, arsenopyrite, pyrrhotite, hematite, magnetite, electrum, enargite, Fe-bearing aikenite (a bismuthian sulfosalt), meneghinite, jordanite, bournonite and rutile (Gifkins et al. 2005; Green et al., 1981). Chlorite, quartz, muscovite and several carbonates are the dominant gangue minerals with minor phases of spessartine, albite and coarse-grained barite (Brathwaite,

1974; Green et al., 1981).

The base of the lenses includes an assemblage rich in pyrite and chalcopyrite that may alternate with phyllosilicate bands in some lenses (Solomon et al., 2004; Zaw et al., 1999). Cu-rich zones are restricted to the base of the lenses, as is free Au (Brathwaite, 1974; Green et al., 1981). Above the base of the lenses sphalerite and galena become enriched and Ag is associated with the base metals (Green et al., 1981).

Barite-rich lenses overlie the ore lenses in some areas of the mine and contain banded barite with sphalerite and galena (Gifkins et al. 2005; (Green et al., 1981; Solomon et al., 2004). Carbonates (mostly Mn-bearing, i.e. rhodochrosite and kutnahorite) can occur as lenses within the ore lenses and beneath the lenses (Brathwaite, 1974; Green et al., 1981; Solomon et al., 2004). The carbonates precipitated contemporaneously with the sulfides whereas other carbonates replaced host rock above and below the ore lenses (Solomon et al., 2004). Reduced acid fluids derived from an underlying Devonian granitoid pluton caused replacement of some lenses sections to pyrrhotite-pyrite and magnetite-biotite-chalcopyrite assemblages south of 100 mS (Solomon et al., 2004; Zaw et al., 1999).

Fine compositional banding (0.1 – 10 cm thick) is a common ore texture (Brathwaite, 1974). Colloform banding and carbonate colloform growths with sulfide rims occur and suggest growth in cavities after ore formation (Green et al., 1981). Metamorphic porphyroblastic textures of pyrite and arsenopyrite occur at the microscopic level within a fine-grained polygonal matrix composed of sphalerite, galena, chalcopyrite, barite and quartz (Green et al., 1981). Other metamorphic textures include pyrite and arsenopyrite cataclastic brecciation and kinked twin lamellae in sphalerite (Green et al., 1981). These metamorphic textures suggest a deformation and annealing history with secondary and differential recrystallisation (Green et al., 1981).

Two stages of Devonian deformation have affected the stacked stratiform ore sheets, producing tight folds and thrust faults (Large et al., 2001). The southern end of the orebody has a complex structure whereas the northern end is less complicated (Large et al., 2001).

Different alteration phases occur in alteration zones around the deposit, extending from the

margin to the core (Gifkins et al., 2005a). These assemblages include a sericite zone, chlorite zone, Mn-carbonate zone and quartz + sericite zone (Gifkins et al., 2005a). Strata-parallel intense quartz + sericite alteration zones are characteristically associated with massive and semi-massive mineralisation (Gifkins et al., 2005a). One interesting feature is that there is no well–developed stringer zone at Rosebery (Large, 1992). Chlorite-pyrite-rich zones are present under more Cu-rich lenses at the southern mine end but no chlorite-rich alteration pipes exist (Large et al., 2001). The chlorite-rich zones may be recording the high-temperature parts of the hydrothermal system (Large et al., 2001). The Rosebery alteration history includes early diagenetic alteration being overprinted by ore-forming hydrothermal alteration. Another alteration assemblage formed during Devonian deformation was finally overprinted by granite-related alteration assemblages (Large et al., 2001).

Previous work interpreted the origin of the Rosebery deposit to be a syn-volcanic exhalative (e.g. Braithwaite, 1974; Green et al., 1981) with later interpretations (Solomon and Groves., 1994) suggesting a high-salinity brine pool similar to SEDEX formation (Gifkins et al., 2005a). The source fluids may have occurred in convection cells of seawater that circulated in the felsic volcanics caused by Cambrian intrusions (Green et al., 1981; Large, 1992). The convection cells, around 49 to 100 km^2 in size, could access metal and sulfur sources at 4 – 5 km depths (Large, 1992). As no stringer zones or alteration pipes are present, lateral fluid flow on the seafloor or sub-seafloor could have occurred (Allen, 1991 unpub.; Gifkins et al., 2005a). Replacement of the permeable fine-grained pumice breccia in the host succession may have occurred below the seafloor (Gifkins et al., 2005a).

2.4.2 Hercules VHMS deposit

The Hercules polymetallic massive sulfide deposit lies 7 km south of Rosebery on the flank of Mt Hamilton (Gifkins et al., 2005a; Lees, 1987). A. E. Conliffe discovered Hercules in 1894 (Gifkins et al., 2005a; Lees, 1987). In 1986, mining ceased and a total of 2.3 Mt was mined at 5.5% Pb, 17.3% Zn, 0.42% Cu, 172 g/t Ag and 2.8 g/t Au (Lees, 1987).

The Hercules mineralisation occurs as several connected lenses that are either sheets or

pods in shape (Lees, 1987). Folding and attenuation of the small (100 x 100 x 5 – 10 m) lenses occurred during the Devonian deformation (Gifkins et al., 2005a). All the lenses are parallel to cleavage, dipping at 70^{o} E, and are oblique to bedding (Lees, 1987). The lenses are zoned in mineralisation; the core is Pb-Zn-rich massive sulfide, surrounded by a siliceous zone, rich in chalcopyrite and pyrite that thins and disappears with depth (Lees, 1987). A halo of carbonate-rich rocks envelopes the Pb-Zn ore lenses and includes packed oolites, recrystallised or massive carbonate or rare colloform carbonate (Lees, 1987). These carbonate features occur around 1 m distance to ore and may be a vector as pink or brown colouring is noted relating to a higher Mn-Fe content (Lees, 1987).

Several ore types can be differentiated from mineralogy and texture (Lees, 1987). The porphyroblastic ore texture is widespread and has a variable in mineralogy and grade throughout the deposit (Lees, 1987). Sphalerite has been recrystallised into 2 – 20 mm porphyroblasts with thin galena rims (Lees, 1987). Pyrite and chalcopyrite are intergrown with the porphyroblasts and between the porphyroblast is a matrix of muscovite, quartz and silicate gangue (Lees, 1987). Spotty ore occurs on the peripheries of the porphyroblastic ore and consists of 2 – 5 mm spheroids to flattened ovate spots (Lees, 1987). These spots consist of sphalerite and galena with muscovite and crystalline quartz rims and outer pyrite rims (Lees, 1987). The sulfide spots may have originated by either infilling of cavities within a vesicular pyroclastic ashy unit or filling of carbonate nodules after dissolution (Lees, 1987). Other minor ore phases include sericitic ore, baritic ore and copper ore (Lees, 1987).

The Hercules deposit resembles other VHMS deposits in the types of ore, the grade, mineralogy, associated rock types and extensive footwall alteration observed (Lees, 1987). However, numerous features including the spotty ore are formed usually by replacement processes or cavity-filling within the pyroclastic host (Lees, 1987). A more in-depth formation interpretation is given below.

The South Hercules deposit lies 1 km south along strike of the Hercules deposit in the same ore horizon (Zaw and Large, 1992). The South Hercules ore lenses are disseminated to semi–massive and contain considerable Au and Ag (Zaw and Large, 1992). South Hercules is thought to occur in similar units to those hosting the Rosebery deposit but

lower in the stratigraphy (Zaw and Large, 1992).

The two main mineralisation and alteration facies of South Hercules are the mineralised sulfide facies and the carbonate facies (Zaw and Large, 1992). A massive pyrite ± barite zone, a siliceous ± stringer sulfide zone and a sphalerite – galena ± pyrite zone compose the mineralised sulfide facies (Zaw and Large, 1992).

The carbonate alteration facies surrounds and interfingers with the upper sulfide facies and includes a blebby carbonate – chlorite zone, a massive carbonate zone and a cherty carbonate zone (Zaw and Large, 1992). The insignificant precious and base metal grades characterise the carbonate facies (Zaw and Large, 1992).

The South Hercules deposit predominantly contains disseminated and stringer mineralisation styles surrounded by extensive carbonate alteration zones that extend into the hangingwall sedimentary and volcanic rocks (Zaw and Large, 1992). These features, together with other geologic, stable isotopes and fluid inclusion data, suggest a sub-seafloor replacement formation process (Zaw and Large, 1992). Low temperature (150^{o} – 250^{o}C) and near neutral fluids are interpreted to be responsible for ore transport and deposition (Zaw and Large, 1992). These fluids could transport Au as bisulfide complexes and the base metals as chloride complexes but would not transport Cu due to the low temperature (Zaw and Large, 1992). The carbonate alteration may have resulted when the moderately acidic ore fluids (pH 4 to 5) evolved to near–neutral fluids (pH 5 to 6) from mixing with seawater in the porous sub-seafloor volcaniclastic units (Zaw and Large, 1992). This process may explain the high Au content as the bisulfide complexes became destabilised from fluid mixing (Zaw and Large, 1992). The South Hercules deposit may indicate a transition toward epithermal Au–Ag mineralisation where a seafloor massive sulfide deposit was fed by a submarine version of an epithermal stockwork (Zaw and Large, 1992).

2.5 Summary

Extensive exploration for potential economic VHMS style mineralisation in the Mt Read Volcanics of western Tasmania is particularly important. The main lithostratigraphic units include the Sticht Range Beds, the Eastern quartz-phyric sequence, the CVC, the Western

volcano-sedimentary sequence and the Tyndall Group. The Rosebery and Hercules deposits are examples of VHMS mineralisation that occur in the Mt Read Volcanics. The White Spur area may host potential deposits similar to these. The White Spur Formation lies at the base of the Dundas Group, which is apart of the Western volcano-sedimentary sequence.

Chapter 3 Geology of White Spur

3.1 Introduction

White Spur lies within the Mt Read Volcanics of western Tasmania and consists of the Western volcano-sedimentary sequence (Dundas Group) and the CVC (Figure 3.1). The contact between these two lithostratigraphic units is an important marker for exploration for VHMS ore deposits similar to the Rosebery and Hercules ore deposits. The Rosebery, Hercules and South Hercules massive sulfide deposits are hosted in the stratigraphic interval, known informally as the Rosebery-Hercules host sequence at the top of the CVC. The characteristics and significance of this sequence will be discussed in detail in chapter 6 but will be introduced in this chapter with relevance to the White Spur stratigraphy.

This chapter discusses the major units (the CVC and White Spur Formation) and the structure of the White Spur area.

3.2 Stratigraphy of White Spur

The stratigraphy of White Spur includes the White Spur Formation at the base of the Dundas Group and the underlying, extensive feldspar – phyric CVC. At White Spur, the CVC consists of pumice breccia and various intrusions that grade upward into stratified siltstone and sandstone considered as host sequence. The feldspar-quartz-phyric volcaniclastic units of the White Spur Formation overlie the host sequence. This succession has been informally grouped into the Rosebery-Hercules host sequence, consisting of; the Footwall Pyroclastics, the Host Rocks, Black Mudstone and the Hangingwall Volcaniclastics (Gifkins, 2001 unpub.). Recent research suggests that the Hangingwall Volcaniclastics are equivalent to the White Spur Formation and that the Footwall Pyroclastics can be further subdivided (McPhie & Allen, 1992).

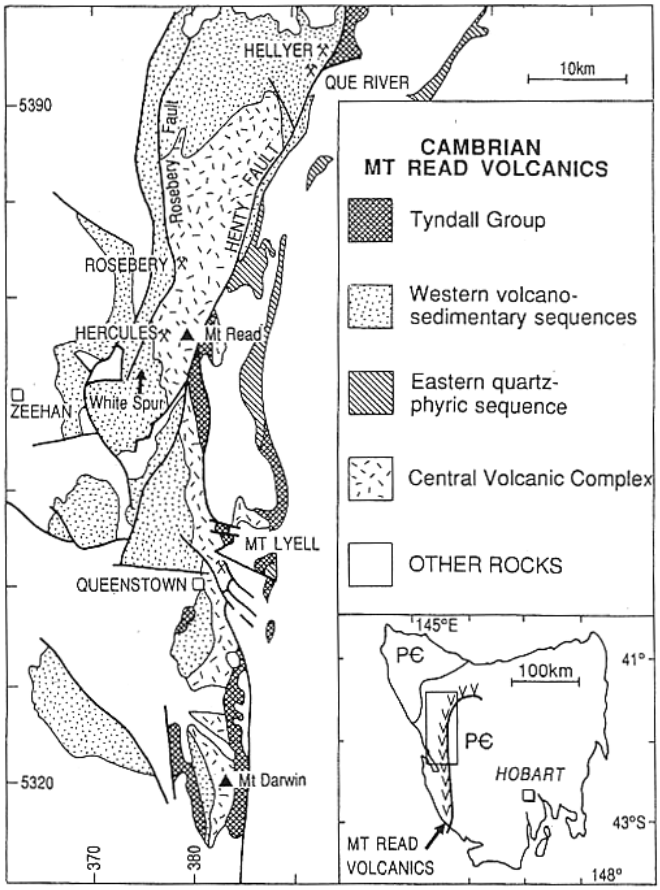

Figure 3.1: Geological map of the central portion of the Mt Read Volcanics highlighting the lithostratigraphic divisions, major massive sulfide deposits and the location of White Spur (From McPhie and Allen, 1992).

3.2.1 The CVC at Hercules

Previously, the northern CVC included the informal units of the Rosebery-Hercules host sequence, the Mt Black Volcanics, the Sterling Valley Volacnics and the Hollway andesite (Figure 3.2; Brathwaite, 1974; Campana & King, 1963; Corbett and Solomon, 1989). The Rosebery-Hercules host sequence was divided into the Footwall Pyroclastics, the Host Rock, black mudstone and the Hangingwall Volcaniclastics (Corbett, 1981; Green et al., 1981; Corbett & Lees, 1987).

It was proposed that the Hangingwall Volcaniclastics and black mudstone are correlates of the White Spur Formation and is apart of the Dundas Group not the CVC (Allen, 1991 unpub.).

Gifkins (2001 unpub.) proposed a formal subdivision of the northern CVC as no attempt had been made on regional stratigraphic subdivisions. This division included the Sterling Valley Volcanics, the Mt Black Formation, the Kershaw Pumice Formation and the Hercules Pumice Formation.

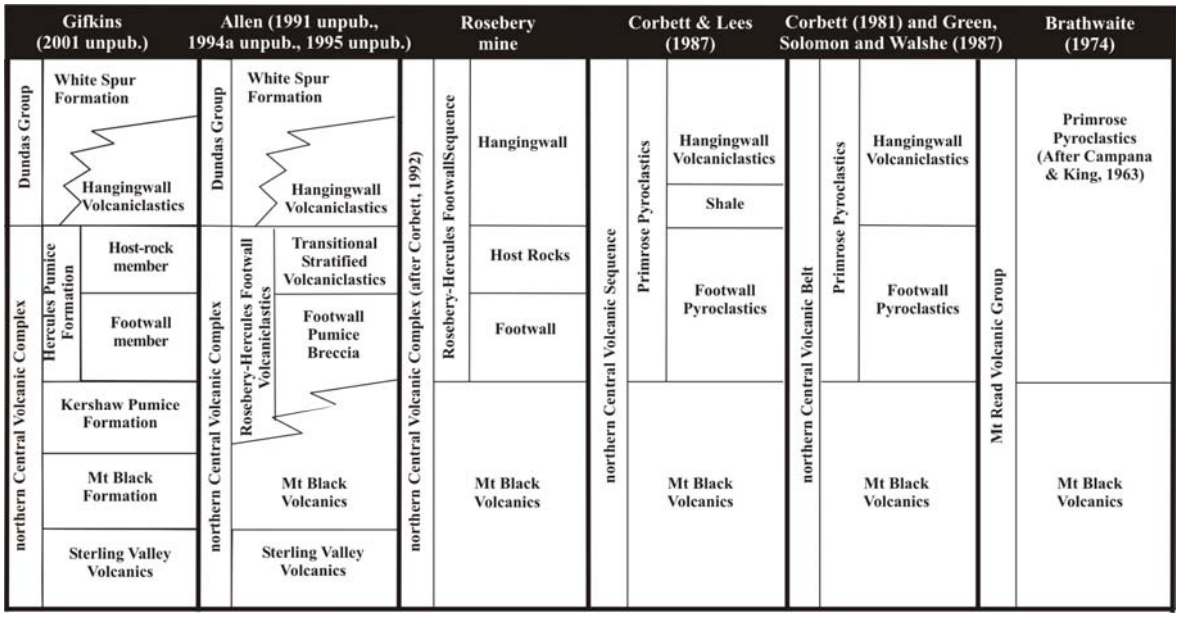

Figure 3.2: Modern and previous stratigraphic subdivisions of the northern CVC. This is not equivalent to a stratigraphic column (Modified from Gifkins, 2005 unpub.).

The pumiceous facies and associated rhyolitic and dacitic lavas and sills of the MRV were formally defined as the Kershaw Pumice Formation (Gifkins, 2001 unpub.). The Footwall Pyroclastics and Host Rocks of the Rosebery-Hercules host sequence were formally assigned to the Hercules Pumice Formation as the Footwall member and the Host-Rock member. The Kershaw Pumice Formation and the Hercules Pumice Formation have been correlated based on facies, structural and lithogeochemical analysis (Gifkins, 2001 unpub.).

The Kershaw and Hercules Pumice Formations are >800 thick and are laterally extensive (>16 km; Gifkins, 2001; Gifkins et al., 2005b). The formations are composed of non-welded feldspar-phyric pumice breccia, pumiceous sandstone and shard-rich siltstone, intercalated with pumice-lithic clast-rich breccia and sandstone, and rhyolitic and dacitic lavas and syn-volcanic intrusions (Gifkins, 2001).

The Hercules Pumice Formation at White Spur includes extremely thick, poorly stratified,

feldspar-phyric rhyolitic-dacitic pumice breccia beds that grade to fine-grained stratified tops. The uppermost stratified intervals are considered the Host Rocks of the Hercules and Rosebery deposits. The pumice beccia extends south to the North Henty fault (Dugdale, 1992 unpub.). Single pumice breccia beds range from 10 m to at least 150 m thick. Numerous depositional units comprise the 800 m thick sequence (Allen and Cas, 1990; McPhie & Allen, 2003). The lower intervals of the beds are moderately sorted and massive. The bases contain rare lithic clasts of feldspar-phyric, spherulitic and amygdaloidal rhyolite and dacite, basalt and crystal-rich sandstone (Gifkins, 2001 unpub.; McPhie & Allen, 2003).

The lower contact of the pumice breccia is not exposed (McPhie & Allen, 2003). Where the top most stratified sandstone is missing, the White Spur Formation overlies the pumice breccia. Minor coherent and brecciated rhyolitic-dacitic facies occur in the CVC throughout the White Spur area (Gifkins, 2001 unpub.).

As stated in the previous chapter, the CVC was deposited in a submarine, below wave base setting. This conclusion is interpreted from the facies types, bedforms and associated VHMS deposits. The extensive pumice breccia beds were produced by a large, felsic explosive eruption. Pumice clasts were transported and deposited by volcaniclastic turbidity currents, debris flows and suspension (Gifkins, 2001 unpub.; McPhie & Allen, 2003).

3.2.2 The Host Rocks

The Host Rocks are a 5–60 m discontinuous layer of graded and/or diffusely thinly stratified rhyolitic pumiceous siltstone and crystal-rich tuffaceous sandstone (Allen & Cas, 1990; Corbett & Solomon, 1989; Gifkins, 2001 unpub.; Large et al., 2001; McPhie & Allen, 2003). These beds grade from the massive pumice breccia beds of the Hercules Pumice Formation. Pumice clasts and shards are the main components of the beds. Feldspar and quartz crystal fragments are also present lying toward the top of the unit (Gifkins, 2001 unpub.).

The Host Rocks consist of pyroclasts generated by distal rhyolitic volcanic centres and transported and deposited by suspension sedimentation and/or by volcaniclastic turbidity

currents (Gifkins, 2001 unpub.). Some components were also possibly reworked from the underlying pumiceous CVC (Allen, 1994a unpub.; Large et al., 2001).

3.2.3 The White Spur Formation

The geology of the Hercules area has been documented by the work by Brathwaite (1974), Corbett (1992), Corbett and Lees (1987), Green et al. (1981), McPhie and Allen (1992), Gifkins (2001 unpub.) and Allen (1991 unpub., 1994a, b unpub.). Corbett and Lees (1987) placed the Rosebery-Hercules host sequence in the White Spur area into the CVC even though they recognised that it was lithologically, compositionally and texturally similar to parts of the Dundas Group (Allen, 1991 unpub.; Gifkins, 2001 unpub.). The Hercules Hangingwall Volcaniclastics are now correlated with the White Spur Formation as recent structural interpretations suggest that they are broadly equivalent (Corbett, 2002).

Corbett and Lees (1987) first described the White Spur Formation as a west-facing sequence of felsic tuff, siltstone, greywacke, and slate that overlies the CVC between the North Henty Fault and Williamsford.

The White Spur Formation is 5–400 m thick and laterally extensive along strike for 13 km (Gifkins, 2001 unpub.; McPhie & Allen, 2003). At Williamsford, the White Spur Formation wedges out against the Rosebery Fault and reappears at Rosebery on the western side of the fault as a 1 km wide belt (Corbett & Lees, 1987; Dugdale, 1992 unpub.). The White Spur Formation extends south to the North Henty Fault. The White Spur Formation is overlain to the west by Precambrian-derived micaceous quartzwacke and conglomerate (Corebtt & Lees, 1987; Corbett, 1992). At Hercules, the White Spur Formation overlies the CVC (Corbett, 1992).

The Hercules Hangingwall Volcaniclastics and the White Spur Formation are both composed of mass-flow deposits including graded, feldspar-quartz-phyric, crystal-rich, pumiceous volcaniclastic sandstone/breccia interbedded with black mudstone and lithic sandstone turbidites (Allen, 1991 unpub.; Corbett; 1992; Corbett & Lees, 1987; Gifkins, 2001 unpub.). Feldspar-phyric rhyolite and dacite and intercalated black mudstone lenses are present in the White Spur Formation (e.g. White Spur; Gifkins, 2001 unpub.). Both successions can be divided into a sediment dominated top and lower volcanic dominant

section (Allen, 1991 unpub.).

In the White Spur Formation, the volcaniclastic breccia-sandstone units can >10 m thick and grade from a breccia base to upper sandstone and siltstone intervals. Pumice clasts (<2–10 cm), crystals (1–2 mm) and shards (<1 mm) are the principal pyroclastic components of the units (McPhie & Allen, 2003). At the stratified top, fine-grained pumice and shard components are concentrated, with the middle dominated by pumice lapilli (McPhie & Allen, 2003).

The basal quartz-feldspar-phyric pumiceous rhyolite breccia bed of the White Spur Formation is concentrated in normally graded, poorly sorted, large dense lithic clasts (Dugdale, 1992 unpub.; Gifkins, 2001 unpub.; McPhie & Allen, 2003). These clasts can be up to several metres across and are of variable volcanic and non-juvenile components (Dugdale, 1992 unpub.; Gifkins, 2001 unpub.; McPhie & Allen, 2003). The lithic clasts include quartz-and/or feldspar-phyric rhyolite, pumice, spherulitic and amygdaloidal dacite, siltstone, sandstone, schist, limestone, and chert together with intra-formational black mudstone clasts and rare granite and massive sulfide lithic clasts (Gifkins, 2001 unpub.; Green et al., 1981). The contact with the underlying black mudstone is locally erosional (Gifkins, 2001 unpub.).

Black mudstone occurs as 5–20 m thick lenses at the base of the White Spur Formation and overlies the Host Rocks and CVC (Gifkins, 2001 unpub.). The black mudstone lenses are associated with the large Rosebery, Hercules and South Hercules VHMS deposits and lie above them at the base of the Hangingwall Volcaniclastics (Gifkins, 2001 unpub.). The mudstone contains pyrite that can be interbedded with quartz-feldspar-phyric siltstone and sandstone that contains quartz-feldspar-phyric Precambrian-derived quartzite and quartz-mica schist clasts (Gifkins, 2001 unpub.).

The well stratified White Spur Formation has been subdivided into 5 separate stratigraphic units by Allen (1991 unpub., 1994a unpub., 1997 unpub.). The 5 units range from 10 cm to 100 m in thickness (Gifkins, 2001 unpub.). Each unit will be described in following chapters in terms of lithofacies, composition, formation and geometry.

These units are interpreted to have formed in relatively deep submarine settings (McPhie &

Allen, 2003). The units were deposited by submarine density currents that interrupted normal sedimentation in distal to medial settings relative to the source vents and possibly caused by a single explosive eruption (Green et al., 1981; McPhie & Allen, 2003).

3.3 Structure and younging directions

Previous workers on the northern Mt Read Volcanics have highlighted problems with structural interpretations in the White Spur area. From Rosebery to White Spur, the White Spur Formation dips and youngs west, and unconformably overlies the east-dipping and younging CVC (Corbett and Lees, 1987; Dugdale, 1992 unpub.; Gifkins, 2001 unpub.).

Corbett and Lees (1987) show that the White Spur Formation at Hercules is west-younging and contains numerous north-south trending folds (Figure 3.3). The Hangingwall Volcaniclastics above Rosebery and Hercules are east-younging (McPhie & Allen, 1992). The Hangingwall Volcaniclastics at Hercules consist of north-south trending folds (Corbett and Lees, 1992). At Mt Hamilton, the Hangingwall Volcaniclastics are overlain by pumice breccias of the Kershaw Pumice Formation emplaced by the Mt Hamilton Fault (Figure 3.4; Corbett, 2002). The implications of the structure of these successions will discussed later in this chapter.

The Host-rock member of the Hercules Pumcie Formation conformably overlies the Footwall member between Rosebery and Hercules (Gifkins, 2001 unpub.). West of Rosebery, the Rosebery Fault is the contact between the Hercules Pumice Formation and the White Spur Formation (Gifkins, 2001 unpub.). The Hangingwall Volcaniclastics and the White Spur Formation overlie the Footwall Member where the Host-rock member is missing (Gifkins, 2001 unpub.).

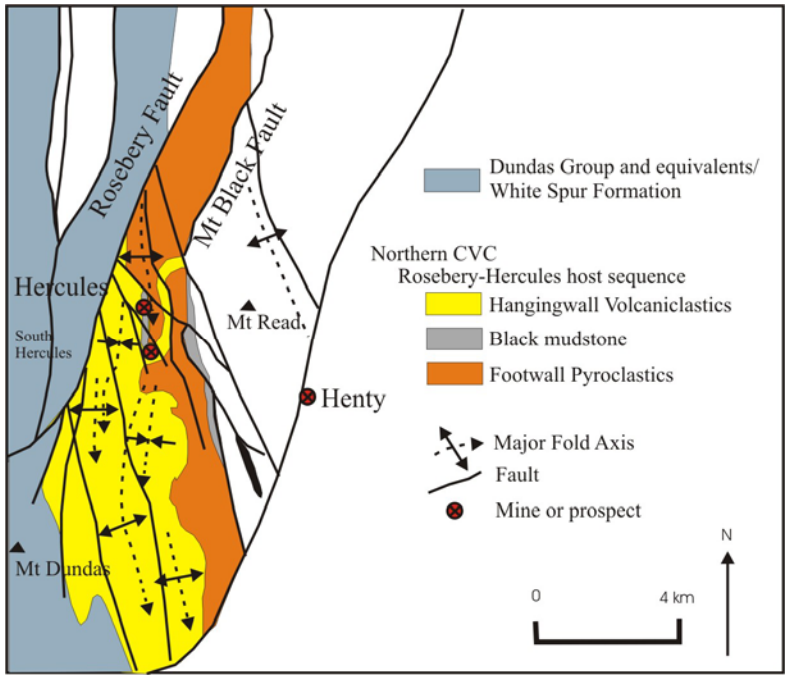

Figure 3.3: Map showing the major lithologies and structural features of the Dundas Group and northern CVC in the Hercules-White Spur area (Modified from Gifkins, 2001 unpub.).

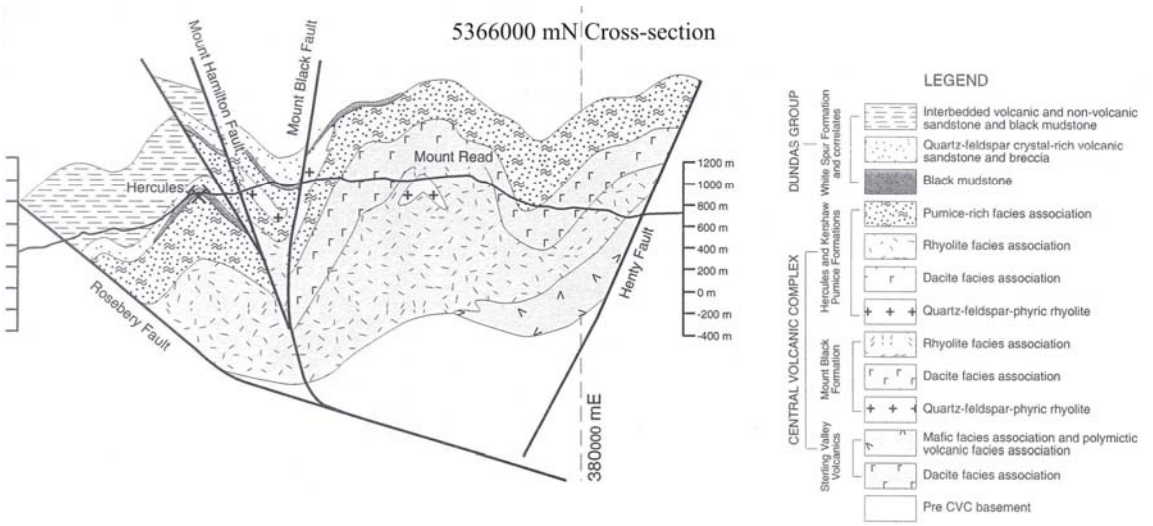

Figure 3.4: Interpretative cross-section through the CVC of Hercules showing major facies associations and structures (Gifkins, 2001 unpub.).

The contact between the White Spur Formation and the CVC at White Spur is contentious. Gifkins (2001 unpub.) believed the contact to be conformable in some areas whereas in other areas, the contact is a folded, low-angle unconformity or disconformity. The contact may either be a paraconformity or a disconformity according to Allen (1991 unpub., 1994a unpub.). Allen (1991 unpub.) believed the contact to be a disconformity offset by faults

and that the White Spur Formation may interfinger with the Hercules Pumcie Formation. McPhie and Allen (1992) speculated that the contact may be an erosional angular unconformity and that a significant time interval was required for uplift and erosion of the CVC prior White Spur Formation deposition.

South of White Spur the contact dips west and shows local topographic relief from the variably steepness in dip (Corbett and Lees, 1987; Dugdale, 1992 unpub.). At Hercules, the White Spur Formation overlies the CVC but the contact relationship is complicated by folding of the CVC about an anticline (Corbett, 1992; Dugdale, 1992 unpub.). This fold is adjacent to the contact and causes the CVC to appear as dipping and younging locally conformably with the White Spur Formation (Corbett, 1992 unpub.).

Previous workers recognised that the Hangingwall Volcaniclastics are very similar to the basal White Spur Formation (Figure 3.5; Corbett, 1992; McPhie & Allen, 1992). The Hangingwall Volcaniclastics and the White Spur Formation were considered as the same unit that had been folded and repeated (Green et al., 1981; Gifkins, 2001 unpub.). At Howards Road and Hall Rivulet Canal, similar facies are repeated by open north-south-trending folds (McPhie & Allen, 1992). The interpretations of the contact relationships between the Hangingwall Volcaniclastics and White Spur Formation included interfingering, or structural emplacement or no relationship exists altogether (Dugdale, 1992 unpub.).

The structural interpretation strongly governs the correlation between the Hangingwall Volcaniclastics and the White Spur Formation (Gifkins, 2001 unpub.). South of Hercules at White Spur, Footwall Pyroclastics pumice breccia equivalents are overlain disconformably by the White Spur Formation (Gifkins, 2001 unpub.). Therefore, the correlation between the Hangingwall Volcaniclastics and the White Spur Formation is broadly correct and the two are likely to be equivalent (Gifkins, 2001 unpub.).

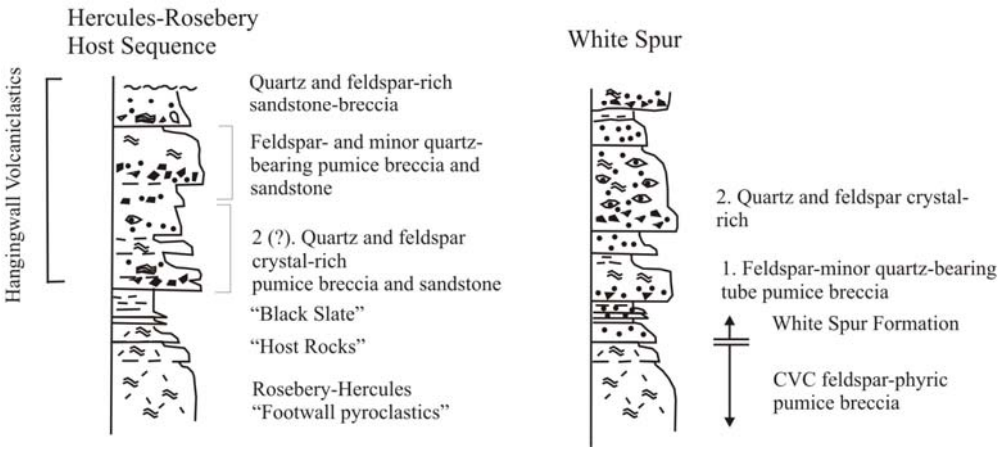

Figure 3.5: Simplified stratigraphic columns showing the lithological similarities between the White Spur stratigraphy and the Rosebery-Hercules Host Sequence (Modified from McPhie & Allen, 1992).

This correlation is possibly apparent from structural and younging information of the White Spur Formation and Hangingwall Volcaniclastics. The White Spur Formation at Hercules and to the southwest is west younging. The Hangingwall Volcaniclastics at Hercules and to the north and northeast are east facing. From this, a broadly general anticline could be interpreted that links the White Spur Formation and Hangingwall Volcaniclastics as correlates on opposing fold limbs.

3.4 Summary

The volcano-sedimentary White Spur Formation consists of feldspar-quartz-phyric pumiceous lithic mass-flow deposits that dip and young west. The CVC is represented by east-dipping and younging, extensive feldspar-phyric pumice breccias of the Hercules Pumice Formation. These thick beds grade into stratified pumiceous crystal-rich siltstone and sandstone referred to as the Host Rocks.

The contact between the White Spur Formation and the CVC is predominantly unconformable. It may be an erosional angular unconformity or a paraconformity.

The Hangingwall Volcaniclastics are believed to be broadly equivalent to the White Spur Formation, due to similarities in lithology, composition, texture and stratigraphic position.

Chapter 4 Volcano-Sedimentary Facies and Stratigraphy of the White Spur Area

4.1 Introduction

The stratigraphy of White Spur was studied with five diamond drillholes and three mapping areas (Figure 4.1). All of the diamond drillholes were collared in the lower White Spur Formation. In this chapter, the facies above and below the CVC and White Spur Formation contact are described by composition, lithology, textures, depositional processes and spatial relationships.

4.2 Principal Facies and Facies Associations in the White Spur Area

The facies at White Spur can be subdivided into the graded volcaniclastic facies, sedimentary facies associations and the felsic facies associations.

4.2.1 Graded Volcaniclastic Facies

This facies includes the graded mass-flow facies of the White Spur Formation and the feldspar-phyric pumice breccia of the CVC.

4.2.1.1 Quartz-Feldspar-Phyric Mass-Flow Facies, White Spur Formation

Crystal – rich mass-flow facies

This mass-flow unit is seen at mapping area 5361453 N and in drillholes DCP 235, WSP 12 and WSP 13 in this study. It is identified as feldspar–quartz–phyric crystal–rich pumiceous polymictic volcanic mass-flow facies. The unit grades from pebble-cobble breccia base through crystal-rich coarse-grained sandstone to volcaniclastic siltstone and fine–grained sandstone top. The unit contains feldspar and quartz crystals along with pumice clasts and numerous types of lithic clasts.

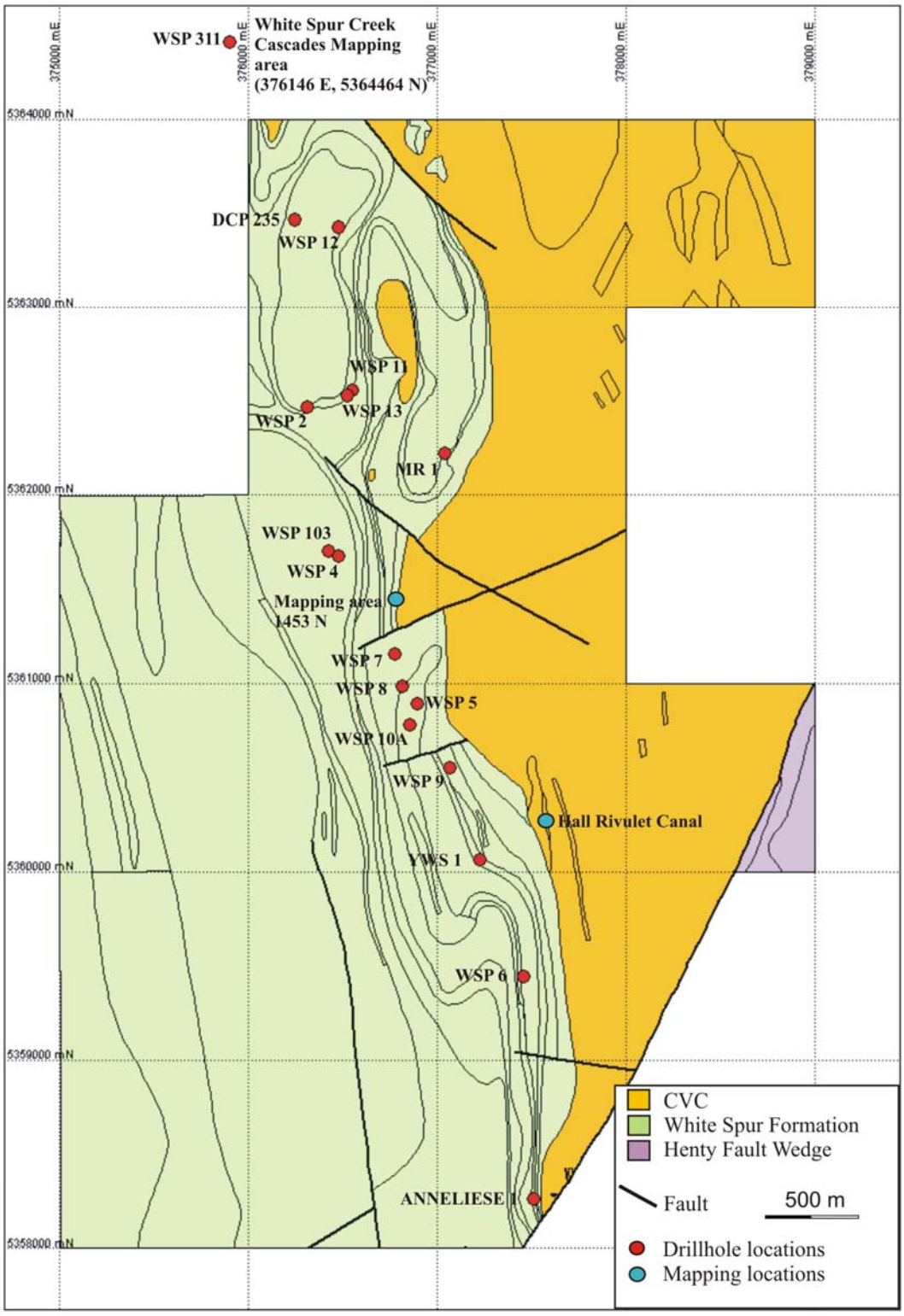

Figure 4.1: Simplified geological map of the White Spur EL 5/96 with locations of drillholes and mapping areas studied.

The upper contact of the facies is graded in DCP 235 and WSP 13 to black mudstone. The upper contact was not exposed in the 1453 N mapping area. In WSP 12, the contact is faulted at ~69 m and black mudstone lies above the 2 m-wide fault zone. Fault contacts occur at the base of the facies in DCP 235 and WSP 13. The contact is conformable in WSP 12 and sharp, irregular and undulating at mapping area 1453 N.

The facies is well-sorted and crystal-rich containing quartz and feldspar crystals that can be fractured (Plate 4.1). The feldspar crystals are 0.5–5 mm, subrounded to subangular and are white, cream or orange. Feldspar makes up 7-15% in the unit and up to 25% closer to the base. Plagioclase feldspar is present as a minor component of the feldspar population. Apple green altered feldspar grains occur and are sericitic or possibly fuchsitic. Carbonate alteration of the feldspars is common. These alteration phases can selectively replace the crystals. The quartz is grey or clear and 0.2–5 mm, subangular to subrounded, and ranges from 5–20%. The very fine matrix (<1 mm) is very crystal-rich and is altered by sericite, carbonate and quartz. Minor leucoxene occurs with the crystals.

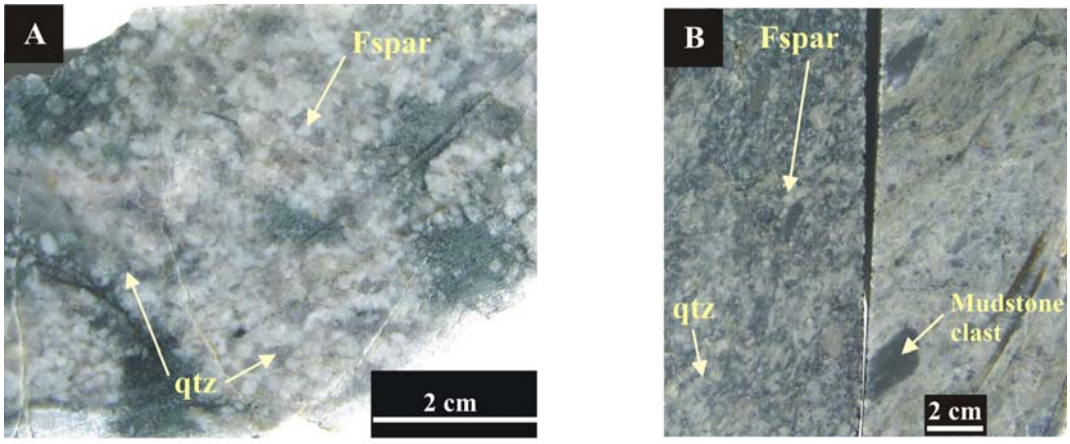

Plate 4.1: (A) Quartz-feldspar-crystal-rich mass-flow unit from WSP 13 at 374 m. (B) Lower basal breccia portion of the crystal-rich mass-flow unit showing mudstone lithic clasts in WSP 13 at 386 m (left) and 407 m (right).

The pumice clasts can be pale green, green brown or black due to sericite alteration or blue to grey due to silicification. The pumice is angular and ranges from 1 mm to 5 cm, and 7% in content. The pumice clasts can also be compacted. Large, up to 20 cm, black phyllosilicate-altered pyrite-rich porphyritic pumice clasts occur in the silicified sandstone

top and cobble breccia base, with 2–5 mm cream, orange or pink subrounded feldspars and 2–5 mm clear quartz crystals.

The most common lithic clast type is 1-8 cm, pale green–cream, porphyritic rhyolite clasts with 1 mm quartz pheoncrysts. Other lithic clasts include blue-grey, subrounded volcanic clasts, cream silicified clasts (5 mm to 3 cm), white subangular volcanic clasts (8 mm), volcaniclastic lithic very fine-grained sandstone clasts (4 cm) with 1 mm quartz crystals, angular grey-cloudy volcanic clasts (1–5 cm), and subangular black mudstone clasts. The mudstone clasts are commonly up to 8 mm but can occur as large intraclasts up to 70 cm that are common toward the basal portion of the facies. The smaller (2 mm) mudstone clasts higher in the facies are elongate and aligned parallel the cleavage. Also, sulfides including 2-5 mm pyrite (?)clasts occur. A 1 cm weathered, sulfide clast occurs around 80 m in WSP 12 with a bright orange halo but this could be alteration of some other clast rather than massive sulfide.

Disseminated pyrite (3%) occurs with orange weathered haloes. Disseminated sphalerite (1%) is present as <1 mm grains. Radiating needle-like pyrite appears on joints with an example at 95.3 m in DCP 235. In DCP 235 at 84.4 m, 85.7–87.4 m and 91 m, laminated ruby red bands and veinlets occur and also as <1 mm disseminated grains. The same mineral occurs in the interbedded facies in the same drillhole (upper DCP 235); this mineral gives the rock a red and pink hue and may be weathered sulfides or red sphalerite. The mineral is unidentified. Minor pyrite and chalcopyrite veins occur with the red mineral at 84.4 m.

Numerous quartz, chlorite, carbonate and sericite veins are common throughout the facies. Some of the veins are anastomosing and sub-parallel to the core axis. The veinlets are evidently cross-cutting in areas. In addition, carbonate spotting occurs throughout the unit. Veins are common with brecciation and small jigsaw-fit breccia zones occur with orange brown $FeCO_3$ infill around fragments.

Massive sulfide clast bearing mass-flow facies

This facies is similar to the previous and grades from a weakly laminated very fine-grained shard-rich volcaniclastic sandstone top to massive, mottled grey and cream, feldspar-

quartz-phyric, pumiceous lithic, medium-grained sandstone and weakly graded very crystal-rich coarse-grained sandstone middle portion and finally to a feldspar-quartz-phyric crystal-rich polymictic pebble-cobble breccia base (Plate 4.2). The facies is seen in WSP 12, WSP 13, WSP 311, 1453 N, and the White Spur Creek Cascades.

The lower contact relationships observed include sharp and undulating conformable contact at WSP 12, WSP 13, WSP 311 and the Cascades (Figure 4.2). This contact is difficult to define at 1453 N due lack of outcrop exposure. Black mudstone underlies the facies except for the Cascades where the CVC pumice breccia occurs. The upper contact is not exposed at the Cascades. The upper contact is gradational in WSP 12 and WSP 13 and sharp, conformable but irregular in WSP 311 and at 1453 N. The overlying facies is the previously described mass-flow facies.

The moderately to well sorted facies contains quartz and feldspar crystals with numerous lithic clast types supported by a microcrystalline matrix of quartz, sericite, chlorite and carbonate. The cleavage is defined by alignment of these minerals. The white, cream feldspar crystals (20%) are usually 1-3 mm and subangular but can occur as laths. These laths are plagioclase feldspar. The feldspar crystals can be brown-green, pink or orange, due to alteration by carbonate and sericite. The common replacement is often intensely selectively but is observed pervasively in areas.

The quartz (10-15%) is clear and subrounded. Some crystals have visible melt inclusions. In WSP 311 at 370–375.3 m, the facies is crystal-rich with 30–40%, subangular to subrounded, white, 1–5 mm feldspar and 10-15%, subrounded, clear, 0.8–8 mm quartz. This is comparable to WSP 13 at 387 m, with 20-25%, 1–5 mm white to cream subangular feldspar and 10-15%, 1–5 mm, clear, subrounded. All the observed crystals are fractured to some extent into smaller fragments by in-situ fracturing.

The lithic clasts include a variety of lithologies with commonly 2-5 cm but occurring 10-30 cm, pale cream, angular porphyritic rhyolite clasts with 1–2 mm, quartz phenocrysts surrounded by silicification haloes (10%). Other minor lithic clast types include 2-4 cm, grey, fine-grained, siliceous, feldspar-phyric volcanic clasts and grey to brown to black, silicified, fine-grained sandstone clasts, 10-30 cm green grey, volcanic siltstone, and 2 mm

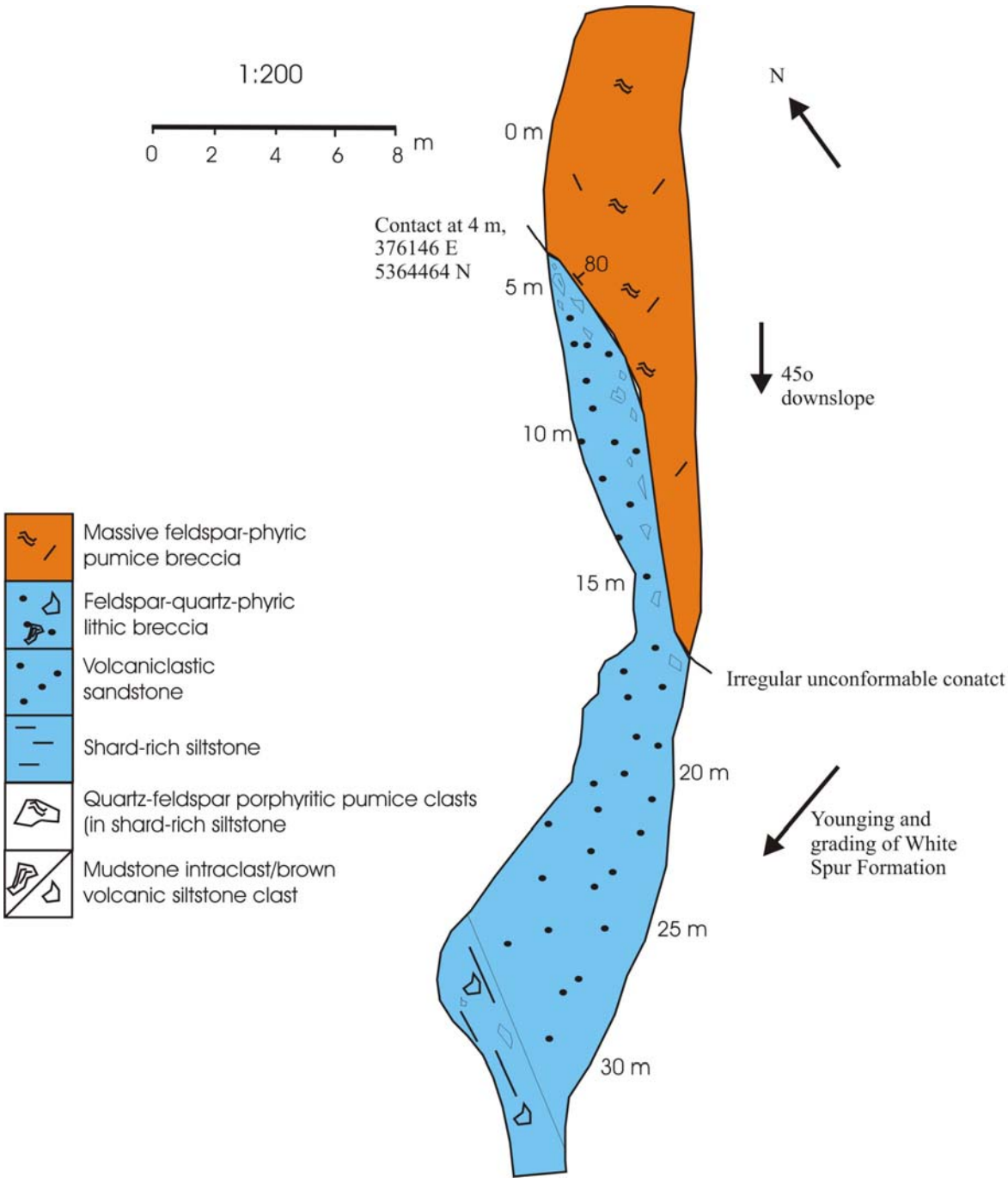

Figure 4.2: Geological map of the White Spur Formation-CVC contact at White Spur Creek Cascades (Modified from Dugdale, 1992 unpub and updated with mapping).

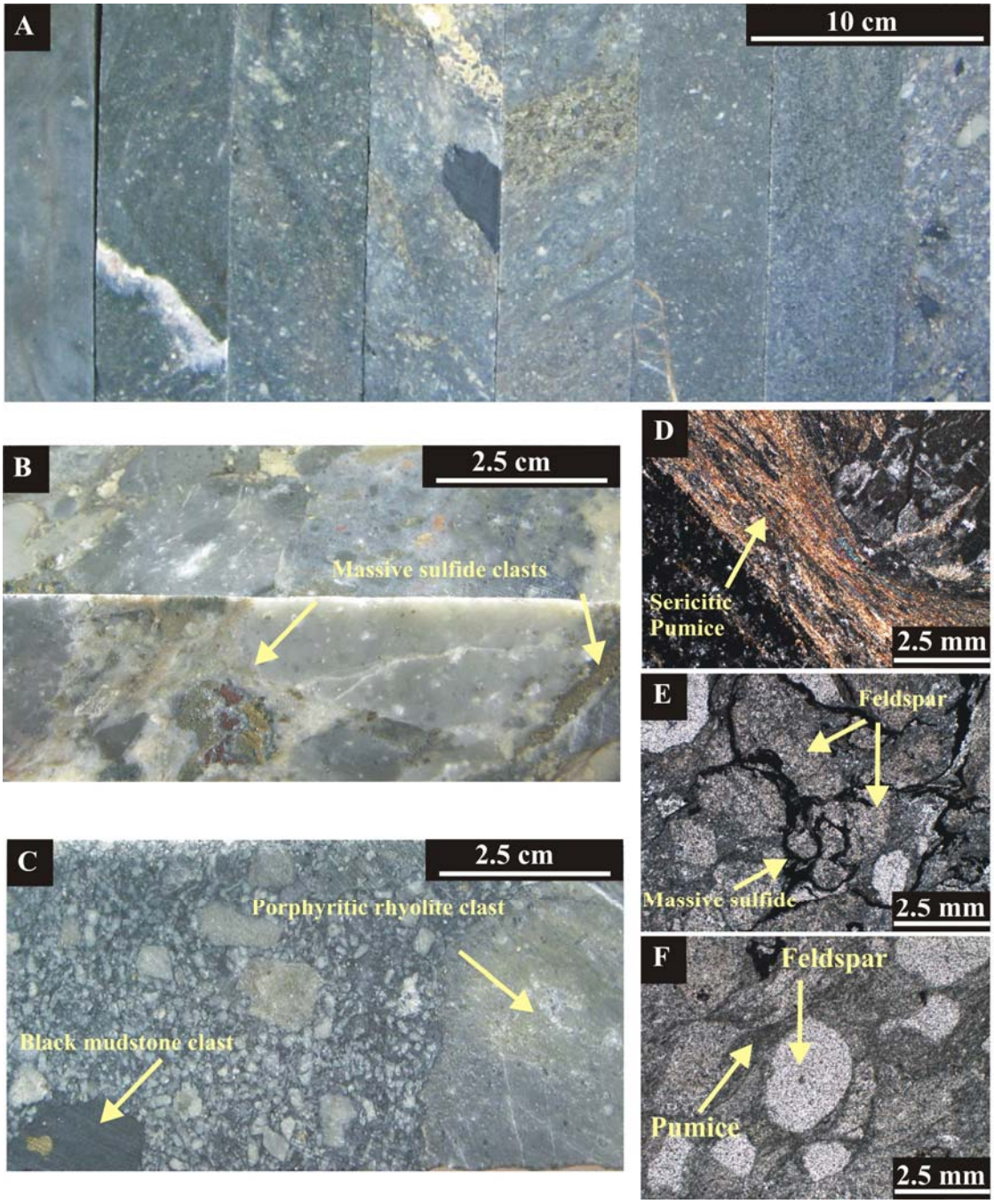

Plate 4.2: (A) The massive sulfide clast-bearing mass-flow unit in WSP 311 from left (119 m), the finer siltstone intervals to right (183 m), through the crystal-rich and lithic-rich sandstone and breccia intervals. (B) The breccia base at 423 m (upper) and 427 m (lower) in WSP 311 with a 1 cm massive sulfide clast of pyrite, sphalerite and galena with an elongate massive pyrite clast to the right. (C) Lithic clast types present in the cobble breccia base at 199 m in WSP 12. (D) Compacted pumice wrapping around crystals in WSP 13 at 423 m (crossed nicols). (E) Massive sulfide present between fractured crystals (WSP 311 at 183 m; PPL). (F) Feldspar crystals with compacted pumice wrapping around the crystals (175 m in WSP 311; PPL).

to 1.5 cm, angular, opalescent cloudy chert clasts. Minor dark green grey, chlorite spotted, andesite clasts are evident. Numerous 2 mm to 30 cm, elongate to angular, black mudstone intraclasts are common, some of which contain quartz and carbonate veins. A clast type exclusive to this facies is <1 cm, blue-grey limestone clasts. These can be subrounded and fossiliferous. Perlitic volcanic clasts are also common only to this facies as well.

Porphyritic pumice clasts (1-5 mm) are common (7%) and are black, green and phyllosilicate and silicic altered, with disseminated sphalerite. The pumice clasts in the siltstone interval occur as small wispy compacted clasts that wrap around other clasts and crystals they are up to 1 mm. Sericitic pumice clasts in the matrix are all aligned defining the cleavage. Shards accompany the pumice in the finer sandstone intervals toward the top of the facies and are altered by sericite, carbonate, quartz and chlorite.

An important lithic clast type in this facies is massive sulfide clast. The clasts can range from 5 mm and greater, the largest seen being 2 cm. Examples occur in WSP 13 at 361.9 m with an 8 mm sphalerite clast, 422.2 m with a sphalerite and pyrite clast, 423.3 m and 428.2 m with a massive pyrite clast. The massive pyrite clast at 423.3 m is elongate (2.5 x 0.2 cm) and aligned with the cleavage. Some clasts are weathered bright orange brown.

Sulfides can occur as disseminated grains. Pyrite is the only sulfide identified as cubic disseminations. The grains can be 1-5 mm and occur as clusters. There is no clear definition between grains and clasts. These 1-3% disseminated sulfides can be weathered red and orange. Other sulfides include sphalerite veins observed in the upper siltstone portion. Pyrite veinlets are associated with brown sericite alteration. Also evident are 1 mm ellipsoidal metallic pods of fine-grained sulfides (3%) that are aligned with the cleavage that is sub-parallel to the core axis. At 183 m in WSP 311, elongate anastomosing sulfides are present around clasts and crystal fragments. It appears the sulfides were compacted around these clasts. Also present at 157 m are small (<1 mm) anastomosing sulfide veinlets that are aligned with sericite and appear compacted between intensely altered clasts.

Irregular fine-grained to medium-grained sandstone beds and pods of 0.5 – 1 mm quartz feldspar and pumice occur in the siltstone tops of the facies. This may be soft sediment deformation causing intermingling of fine-grained sandstone within the siltstone interval.

The common mottled blue-grey to brown silicification of the facies occurs as intense equant patches confusing clast types with alteration artefacts. Pyrrhotite alteration is noticed in areas. Pervasive carbonate is also a major alteration phase. Opaque leucoxene is evident (1%), associated with sulfide occurrence, and can be bladed in veinlets. Minor isolated <<1 mm epidote grains (<1%) occur due to regional alteration overprinting.

The facies contains quartz, sericite, chlorite, carbonate and $FeCO_3$ veins. These can be deformed veins and irregularly shaped or cross-cutting or commonly are anastomosing sub-parallel veining creating a pseudobreccia texture.

Poorly bedded breccia facies

In WSP 10, a crystal-pumice-lithic mass-flow unit is represented by a poorly bedded feldspar-quartz-phyric pumiceous lithic granule-pebble breccia to cobble breccia. There are three main beds 4 to 6 m in thickness between 303.7–329.1 m and separated by intervals of the laminated pyritic black mudstone facies. The 60 cm mudstone layer above the first breccia bed at 303.1–303.7 m contains (?)Devonian pyrrhotite with pyrite, chalcopyrite and minor molybdenite veins with carbonate. The mudstone interval is heavily veined and contains distorted crystals and pumice. The contact between the mudstone and the breccia is very irregular. Flame structures are at the lower contact of the first bed and the lower mudstone. Below the breccia is also laminated pyritic black mudstone.

The well sorted breccia beds contain feldspar and quartz crystals. The feldspar crystals are subrounded to subangular and 1-3 mm with a minority identifiable as plagioclase laths. The feldspar can reach an abundance of 40%. The crystals can be pervasively altered by sericite and to a lesser extent carbonate. The quartz is 1–2 mm and subangular (10–15%).

Lithic clasts include pumice, angular black mudstone clasts, limestone and 3 mm massive sulfide. The clasts can be sericite altered. At the base of the bed, the mudstone clasts are aligned parallel to bedding. At 328.6 m in WSP 10, the breccia bed becomes darker, possibly due to an increase in fine black mudstone clasts.

The crystals and lithic clasts sit in a fine microcrystalline matrix of <1 mm of quartz,

carbonate and sericite. The matrix is shard-rich in the upper sandy intervals. Evidently, the hook-shaped shards appear to be altered by sulfides.

Sulfides occur as 1 mm euhedral disseminated grains (1-3%) but commonly have a ragged and irregular appearance. Brown staining occurs in the matrix caused by sericite and carbonate alteration. Epidote is rare but occurs as isolated grains in addition to small (0.1 mm) euhedral, strawy biotite grains. Carbonate veinlets are common throughout the facies. Styolites composed of opaque phases occur in some parts of the facies. Leucoxene is present as patches (3–5%). This facies is very similar in WSP 10A.

In WSP 311, the massive sulfide clast bearing mass-flow occurs from 0–61 m and shows similar grading to that of WSP 10. The beds can be moderately sorted, matrix supported, and well-graded that grade from pebble to granule grainsize. This facies can be referred to as poorly bedded feldspar-quartz-phyric pumiceous lithic medium to coarse-grained sandstone to pebble-granule breccia.

The pink, cream, white to brown feldspar crystals are 2 mm and subrounded to subangular (15–25%). The feldspars are commonly selectively altered to phyllosilicates such as sericite and minor chlorite and biotite plus carbonate. The feldspars can occur as plagioclase feldspar laths. The quartz crystals are subrounded and 1–2 mm (5–7%). The quartz may occur as clusters of smaller crystals.

Lithic clasts include 5 mm to 3 cm subangular to subrounded black mudstone, fossiliferous limestone, white angular volcanic clasts, blue-grey silicified clasts, 1 mm silicified wispy pumice, dark green sandstone (seen in the Hall Rivulet Canal) and 5 mm massive sulfide clasts. The most common clast type (15%) is 1 cm subrounded cream weakly porphyritic rhyolite, At 45.2 m, a 2 cm cream, silicified, brecciated rhyolite clast is present. The fossiliferous limestone clasts are characteristic of the unit. Typically, the limestone clast are 5 mm and are silica-altered. This alteration preserves the internal textures of the clasts and consequently preserves any fossils present. Identifiable fossils include 1 mm hook-like structures presumably trilobite remains. Importantly, up to 7 mm perlitic volcanic clasts are evident in the facies. The perlite kernels are infilled by silica and the surrounding fractures are sericitic.

The microcrystalline matrix consists predominantly consists of sericitic pumice that defines the cleavage along with other hydrothermal alteration minerals such as quartz and carbonate with minor regional metamorphic biotite and epidote.

Disseminated 1 mm pyrite grains (1%) are rimmed by bright orange weathering halo. The massive sulfide clasts are rimmed by chlorite and are associated with leucoxene. Also minor sulfide veining occurs in the facies. The facies has a mottled pale pink, pale cream and grey green appearance. Chlorite and sericite alteration assemblages are common with $FeCO_3$ veinlets and minor epidote and biotite. Leucoxene occurs as disseminated patches (2–3 %) associated with sufide and other lithic clast types such as the weakly porphyritic rhyolite clasts.

Interpretation of the Quartz-Feldspar-Phyric Mass-flow Facies

The mass-flow facies are interpreted to be deposits from water-supported pyroclast-rich turbidity currents generated in subaqueous settings at medial to distal sites (e.g. McPhie & Allen, 2003; Lowe, 1982). Interstitial fluid turbulence suspended the finer particles while traction and saltation processes transported denser particles at the base of the flow (e.g. Choux et al., 2004; Lowe, 1982).

The extensive and very thick, massive to graded beds reflect the large volume and high supply rate of the gravity currents (c.f. McPhie & Allen, 2003). The lower, massive or weakly graded, thicker and coarser intervals may relate to an initial high–particle concentration, waxing phase of the current and the upper diffusely thinly bedded, thinner and finer intervals relate to the trailing dilute and turbulent, waning phase of the flow (McPhie & Allen, 2003). The poorly bedded breccia facies may have become channelised, concentrateding coarser material. The breccia beds are interbedded with black mudstone, implying the sudden occurrence of a gravity flow during normal ambient sedimentation processes.

Volcaniclastic mass-flows can result directly from eruptions or by redeposition of non-welded debris (McPhie & Allen, 2003; McPhie & Allen, 1992).

Non–juvenile, intrabasinal sedimentary clasts become incorporated into the gravity currents as they pass across wet substrates of mud and sand (i.e. black mudstone

intraclasts). Uncertain clast origins from within the basin include the limestone clasts, the variety of volcanic clasts and importantly, the massive sulfide clasts.

4.2.1.2 Feldspar-Phyric Pumice Breccia, CVC

The feldspar-phyric pumice breccia is a voluminous and extensive facies of the CVC in the Rosebery-Hercules area. It is present in all drillholes and outcrops logged. The facies is generally massive, moderately sorted and very thickly bedded. The massive beds range from 5 to >100 m thick. The pumice breccia can grade into stratified sandstone that marks the contact between the CVC and White Spur Formation (e.g. WSP 13 and WSP 311). The clast size of the pumice breccia ranges from granule breccia to pebble-cobble breccia (e.g. 2–5 mm in WSP 12, WSP 13, DCP 235 and all outcrops and 20–25 mm in WSP 311 and reaching 64 mm in WSP 10 A).

The lower contact of the pumice breccia is not exposed in any of the drillholes or outcrops. In drillholes WSP 12 and DCP 235, the pumice breccia lies under a quartz-feldspar-phyric rhyolite sill with peperitic margins also seen in the Hall Rivulet Canal. WSP 13 and WSP 311 have gradational contacts to stratified fine-grained sandstone containing feldspar-quartz-phyric pumice clasts (the Host Rock). The pumice breccia in WSP 311 has pyritic black mudstone with pumice clasts above it, similar to the WSP 10A footwall contact. WSP 10A has a 15 m interval of unusual poorly sorted monomictic pumice breccia related to the underlying dacitic facies. This pumice breccia has an upper intermingling contact with grey mudstone and thin sandstone beds with large porphyritic pumice clasts.

For such a large unit, the small-scale features of the pumice breccia are quite variable in the White Spur area (Plate 4.3). Feldspar is the only volcanic crystal present and it is randomly oriented and can be equant and prismatic or occur as laths. Feldspar crystals are mainly 1 – 4 mm in size. The feldspar abundance ranges from 10–20% over the whole facies. A small proportion can be identified as plagioclase feldspar. The feldspar crystals range from dominantly subrounded to subangular crystals in all the holes. Rarely, crystals seem intact and equant or euhedral as noticed in WSP 12. Most crystals are fractured into jigsaw-fit fragments seen by hand lens or thin section. The feldspar crystals are white or cream and depending on the alteration styles: apple green (?fuchsitic, sericitic), brown or orange (Fe-rich minerals or muscovite), pink (secondary feldspar with hematite dusting),

cloudy white (silica or secondary feldspar) or colourless (carbonate). These alteration phases vary in intensity from unaltered crystals to murky patches of sericite, sphene and carbonate that reveal the crystal outline and former existence of interlocking feldspar crystals.

The tube pumice clasts are irregular and wispy in appearance and can be porphyritic. The clasts are 1 – 2 mm and can reach 1m (WSP 12), a visible 30 cm clast occurs at 317.5 m in WSP 12. The pumice content can be 95% of the unit. The pumice can be compacted into fiamme and defines a foliation possibly parallel to S_o (e.g. TS 12299). The flattened pumice fiamme are uniformly 7% abundant in the pumice breccia. Round uncompacted vesicles occur at the edges of feldspar. The round vesicles are outlined by fine-grained sericite and are infilled by secondary feldspar and epidote that radiate outward. They were infilled similar to amygdales at a very early stage preventing compaction. The more common compacted pumice can be black, brown or green due to phyllosilicate alteration (i.e. chlorite and sericite) but can be pale due to silicification. Anastomosing sericitic seams define the cleavage throughout the unit. Sericitic and silicified altered pumice are present and change to chlorite in the pink secondary feldspar and chlorite zone lower in the facies.

Several lithic clast types occur in the pumice breccia as minor constituents (5%). Angular black mudstone clasts (~1%) occur in WSP 311 (1–2 cm) and DCP 235 (1–2 mm). Other minor pale to orange volcanic clasts and blue-grey opalescent volcanic lithic clasts are present. The main lithic clast type is subrounded to subangular cream quartz-feldspar-phyric rhyolite. The sizes are 8 mm in WSP 12, 1 cm in WSP 13 and 4 cm in DCP 235. The quartz and feldspar crystals within the clasts are 2 mm.

Small amounts of sulfides do occur in the pumice breccia as disseminated pyrite and sphalerite grains around 1–3% and locally 5% or more. Pyrite occurs more than sphalerite, which is much more abundant than galena. Pyrite grains can be 1–3 mm in WSP 12 and WSP 13 and pyrite bands occur at 526 m and 531 m in WSP 13. In WSP 13, <1 mm black shiny grains are present and also in WSP 12 at 0.5–1 mm. These are clusters of extremely

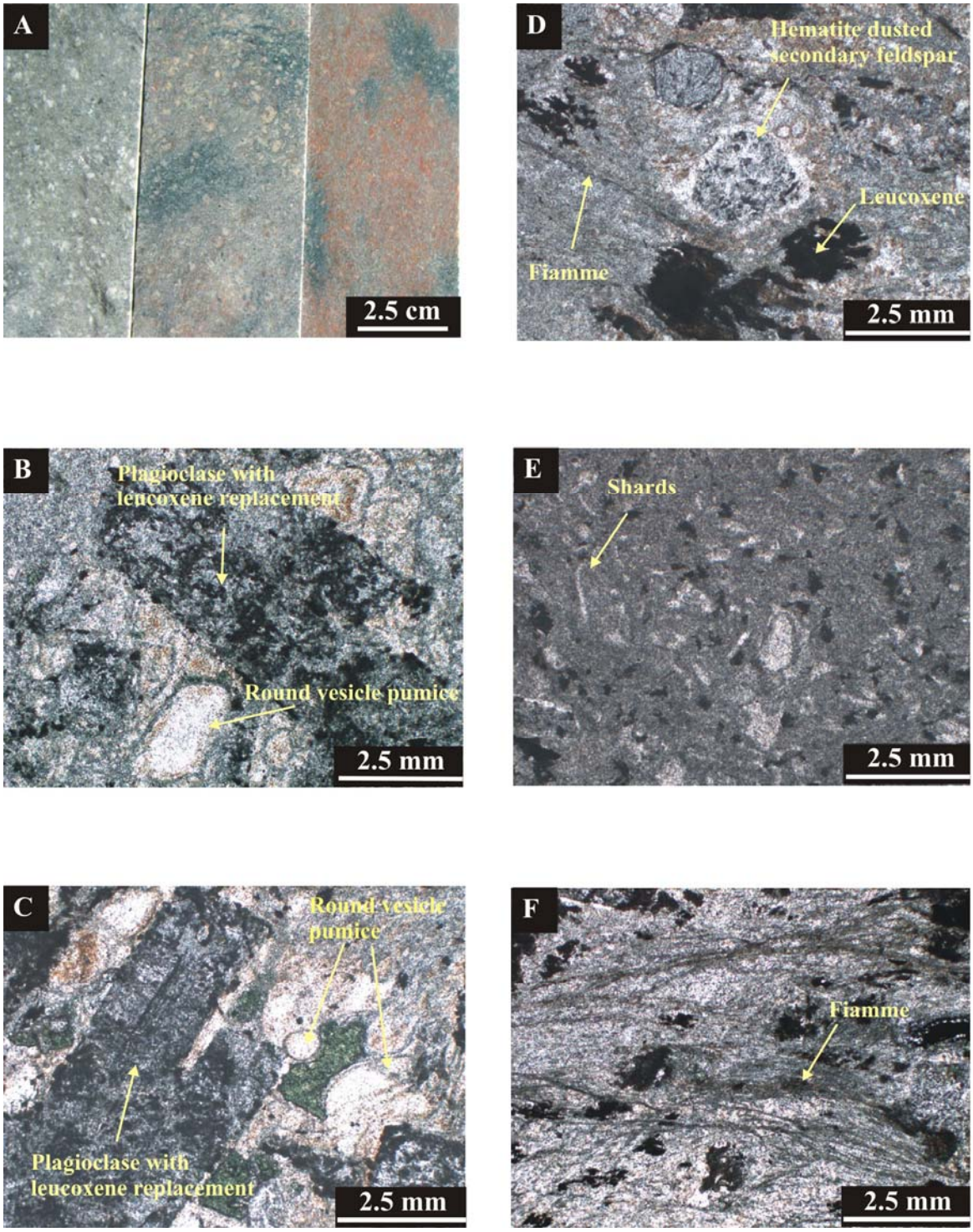

Plate 4.3: (A) The pumice breccia in WSP 12 from 252 m (left) to 299 m (right). (B) Pumice breccia at 426 m in DCP 235, round vesicles around the edges of remnant feldspar crystals. (C) as is (B), several round vesicles surrounding feldspar. (D) Hematite altered feldspar with fiamme flowing around crystals in WSP 12 at 299 m. (E) Shard-rich pumice sandstone bed at EOH (353 m) in WSP 12 with hook shaped shards. (F) Compacted fiamme within pumice breccia in WSP 12 at 299 m. Photomicrographs B-F are PPL.

fine-grained pyrite and sphalerite. These aggregates are subround at the EOH of WSP 12 where 1–3 mm grains of pyrite and sphalerite occur (3%). Honey coloured sphalerite seen in opaque phases (e.g. TS 311221).

The main alteration styles include phyllosilicate (sericite, chlorite), silica and hematite dusted secondary feldspar. Silicification appears as mottled cream white and medium grey greenish or blue grey domains. Intense pink secondary feldspar with hematite dusting and dark green to black chlorite mottling are present and can occur suddenly or gradually. This alteration assemblage occurs mostly in the deeper parts of the CVC and is distinctive of CVC pumice breccia alteration. The pink secondary feldspar and chlorite alteration is selective but pervasive and varies in intensity from weak to strong. Very intense pervasive salmon pink secondary feldspar alteration occurs at 319–320 m in WSP 12. This alteration can have a mottled diffuse banded appearance. Carbonate spotting occurs as <1 mm spots throughout the pumice breccia.

Quartz can occur as rims around feldspars and in vesicles. Epidote is present as a minor phase and possibly a product of from regional metamorphism. Leucoxene is present throughout the entire unit and is usually opaque but can be grey or brown.

The vein styles in the pumice breccia include $FeCO_3$, carbonate and quartz veinlets. They can be sub-parallel to the core axis as at 251 m in WSP 12 or cross-cutting as in WSP 13. Abundant chlorite veins occur in intense pink secondary feldspar alteration at 319 m in WSP 12. Hydraulic fracturing occurs in some locations and is minor but can be 30 cm thick. An example occurs at 487 m in WSP 13 with chlorite infill and veins. The red brown $FeCO_3$ seen in veinlets also appears on fractures and joints that are abundant in the pumice breccia.

In WSP 13 and WSP 311, 1-7 m pumiceous stratified coarse-grained sandstone beds are present and associated with green cream, banded, volcanic siltstone intervals that contain chlorite or sericite altered up to 10 cm porphyritic pumice clasts. This interval is the Host Rock. The feldspar is white, subangular to subrounded and 0.5–3 mm. The pumice is silicified and sericitic. The beds are diffusely banded and mottled green cream and can be altered by blue grey silicification with carbonate spotting and sericite alteration.

Disseminated sphalerite and pyrite (1 mm) is evident in this interval (3%).

In WSP 10A, the Host Rock occurs as a 4 m interval of mineralised grey siltstone with large porphyritic pumice clasts. This interval was logged at a more detailed 1:20 scale (Figure 4.3). It contains pyrite and sphalerite laminations and banding (3%). The greatest amount of mingling occurs beneath the pumice clasts. The pumice clasts are black phyllosilicate altered and have a wispy appearance. The pumice clasts (1-30 cm) have irregular and disrupted sphalerite laminations lying beneath the clasts. The higher concentrations of sphalerite occur at the mingled contacts. The sphalerite has a wispy appearance and could be possibly replacing pumice. Elongate pyrite blebs and coarse 1 cm pyrite grains can occur with pyrite laminations. Sphalerite also occurs in clusters and as disseminated grains (2 mm). At 424.6 m, many 1–2 mm altered pumice clasts occur in the mudstone. The siltstone is overlain by stratified feldspar-quartz-phyric sandstone.

At the base of the pumice breccia in WSP 12 (353 m), a shard-rich fine-grained sandstone bed occurs. The thickness of the unit is uncertain but is approximated at 10-15 m thick. The feldspar appears as 0.5–2 mm randomly orientated laths. This bed contains numerous shards that are 0.5-2 mm. Small (<1 mm) opaque laths are common but were not identified. The bed is silicified and contains fewer crystals compared to the massive pumice breccia beds. Patchy pervasive opaque leucoxene (2-3%) is evident. Disseminated sphalerite and pyrite occur as 1-3 mm grains (3%). The matrix is composed of very fine (<<0.1 mm) sericite and silica. It is possible this bed is the graded top of an underlying pumice breccia bed.

Interpretation of the Feldspar-Phyric Pumice Breccia

The non-welded pumice breccia was produced by an explosive silicic eruption of large magnitude (>10 km^3) (Allen & Cas, 1990; Gifkins, 2001 unpub.; McPhie & Allen, 2003). The beds were deposited on the seafloor in a relatively deep water setting by water supported volcaniclastic gravity flows of high particle concentration and water settling and were synchronous with a major pyroclastic eruption (Gifkins & Allen, 2001). The eruption probably took place from a submarine vent below wave-base with little reworking (Gifkins, 2001 unpub.). The pumice breccia may be an intracaldera facies and is similar in characteristics of subaerial equivalents but lacks hot emplacement textures such as

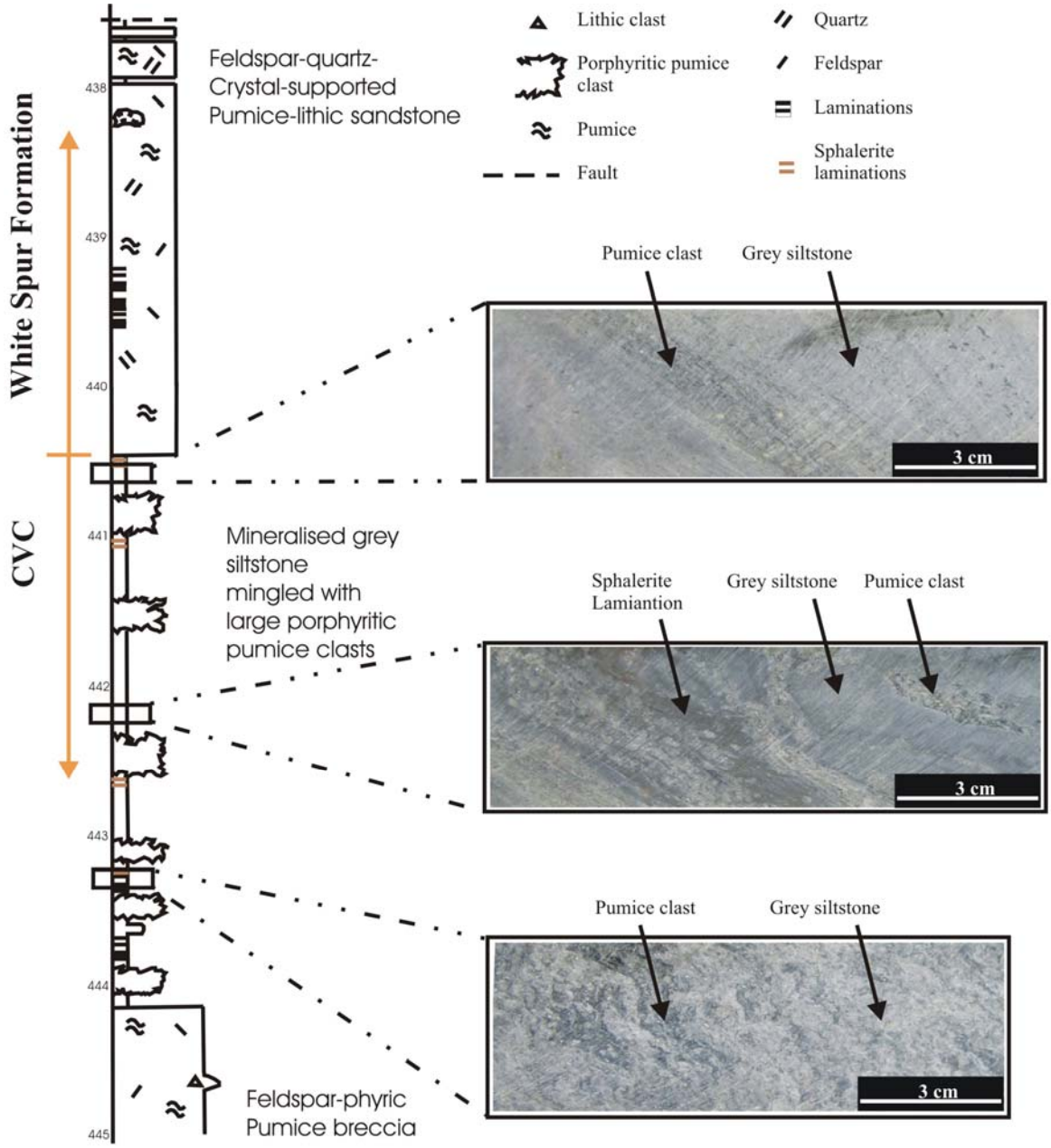

Figure 4.3: The Host Rock interval below the White Spur Formation contact in WSP 10A. Sphalerite laminations are evident below large pumice clasts intermingled with grey siltstone (Logged at 1:20 scale).

welding compaction, columnar jointing and gas-escape structures that other ancient submarine intracaldera successions show (Allen & Cas, 1990).

Highly explosive felsic eruptions are likely at water depths of <1 km and even more so at <500 m (Cas, 1992). Therefore, the vents for the pumice breccia forming eruption may have been at <500 m depth (Gifkins, 2001 unpub.).

4.2.2 Sedimentary Facies Association

This sub-division includes all the lithofacies that contain textures and structures of sedimentary origins. No directly related volcanic influence was involved in the formation of these facies although some contain clasts of volcanic origin. The association includes the laminated pyritic black mudstone facies and the interbedded mudstone and sandstone turbidite facies.

4.2.2.1 Laminated Pyritic Black Mudstone Facies

The laminated pyritic black mudstone facies occurs in all drillholes and outcrops studied except the White Spur Creek Cascades outcrop. The mudstone contains laminations of predominantly pyrite with minor sphalerite. Lithic and feldspar-quartz crystal-rich fine to coarse grained sandstone turbidite interbeds occur as laminations or beds that can be 5 m thick. In total, the sandstone is minor in the facies. The facies includes minor amounts of grey mudstone.

The upper contact of the intervals of black mudstone can either be faulted (DCP 235 and WSP 10), conformable (WSP 311, 12 and 13) or unidentifiable (1453 mN). The lower contact is represented in most of the studied drillholes and outcrops as a sharp conformable contact. An exception is the WSP 10A lower contact, described further below. The lower contact in DCP 235 and WSP 12 is obscured by alteration. The contact is unidentifiable at 1453 N due to limited outcrop exposure. The lower contacts are associated with large porphyritic pumice clasts.

The sulfides in the mudstone include in order of abundance pyrite, sphalerite, galena and pyrrhotite. The pyrite occurs as bands or disseminations that are 5% and can be 10% in parts of WSP 311. The disseminated grains and blebs can be 0.5–3 mm. Interestingly, a 1-cm galena clast occurs in DCP 235 with fine (<1 mm) black sulfide spotting that consists of very fine sulfide grains clustered in aggregates. The large porphyritic pumice clasts present at the lower contact in some of the drillholes contain galena, sphalerite and pyrite bands.

The lower contact of WSP 10A is marked by porphyritic pumice clasts in, and mingled

with the sulfide-bearing grey mudstone (the Host Rock). This contact is described above.

Veins of quartz, brown and orange $FeCO_3$, white carbonate and weathered orange sulfide are common in the facies. Minor vein phases include assemblages of chlorite, pyrrhotite and pyrite, carbonate and chalcopyrite. This assemblage is typical of Devonian veins. The veins can be deformed and irregular, or parallel to bedding, or related to minor hydrothermal brecciation.

Interpretation of the Laminated Pyritic Black Mudstone Facies

Black mudstone forms in quiet water with limited circulation and anaerobic conditions. The laminations and pyrite content suggest anoxic conditions for deposition (Lash and Blood, 2004). The sediment accumulated under SO_4^{2-} reducing, O_2 depleted bottom-water conditions (Piper and Perkins, 2004). Deposition of sediment occurred by suspension and turbidity currents and accumulated in a basin (Pickering et al., 1989). The accumulation of black iron sulfides, volcanic and organic matter gives the black colouration (e.g. Lash and Blood, 2004; Pickering et al. 1989). The water can be O_2 depleted due to weak bottom-water circulation within a basin that is partially isolated from major ocean-boundary currents (Piper and Perkins, 2004).

4.2.2.2 Interbedded Mudstone and Sandstone Turbidite Facies

This facies occurs in WSP 12, WSP 13 and DCP 235. It consists of a lower interval of dark-grey to black mudstone that becomes interbedded with normally graded feldspar-quartz-lithic fine-grained to medium-grained sandstone (Plate 4.4). The thickness of the facies is 50 m in DCP 235, at least 50 m in WSP 12, and 170 m in WSP 13. A typical bed is represented with a mudstone top that grades into a well-sorted lithic sandstone base steadily over tens of centimetres or rapidly into sandstone laminae. Some of the contacts contain flame and lobe structures, showing stratigraphic younging direction, in this case being uphole. At 160 m in WSP 13, a transition to predominantly sandstone facies with mudstone laminae occurs.

The mineralogy of the basal sandstone beds and laminae is uniform throughout the facies. They contain 0.5–1 mm, white, subangular feldspar that is altered by sericite and carbonate and 0.5–0.8 mm, clear–grey, subrounded quartz crystals (10%) in a pumiceous and

shard-rich matrix altered by sericite, carbonate and predominantly quartz. The sericite has altered the 1–4 mm the pumice that is flattened and larger clasts can be porphyritic. Clusters of 2–3 mm subrounded quartz and feldspar crystals occur (originally apart of a larger pumice clast) with 5 mm black pumice.

In hand sample, the lithic clasts include subangular-angular mudstone clasts (2–3 cm), subrounded unidentified brown clasts, blue-grey volcanic clasts and white opalescent volcanic clasts. In thin section, most of the lithic clasts are very fine–grained sedimentary clasts, some more quartz-rich and coarser being very fine–grained sandstone clasts. Several clasts show a previous weak cleavage. The clasts are affected by the strong cleavage.

Other clasts include porphyritic rhyolite and small (2-3 mm) intermediate to mafic igneous clasts composed of fine–grained interlocking plagioclase laths. These clasts show carbonate altered prismatic grains that were ferromagnesian (olivine or pyroxene) in a fine interlocking plagioclase lath groundmass. The lath work in the intermediate to mafic clasts seems undeformed. Felsic and intermediate equigranular clasts are also present.

Granitoid clasts occur with large quartz phenocrysts in a very fine interlocking plagioclase lath groundmass. A carbonate clast is evident with internal concentric structures (?fossiliferous). A 4 mm metamorphic clast contains quartz and carbonate veins that terminate at the clast boundary. This clast is possibly derived from the basement rock of the Tyennan Region. All the clasts and crystals in the sandstone intervals are well sorted and angular suggesting limited re-working has occurred.

Pyrite occurs as 2 mm disseminated cubic-euhedral grains and laminated 1 mm pyrite bands (5-7%). Numerous sphalerite bands and large 1–2 cm sphalerite and pyrite clasts occur. The sulfides occur as laminae, veinlets, and blebs and disseminated grains that can be very large (cm) or small 1 mm fine-grained sulfide aggregates. Ruby red shiny grains, likely weathered sulfides are present in veinlets seen occasionally for example in DCP 235. This mineral is identical in appearance to the mineral observed in the crystal-rich mass flow unit in DCP 235. Isolated 0.5 mm ragged leucoxene patches (1%) are associated with the pyrite.

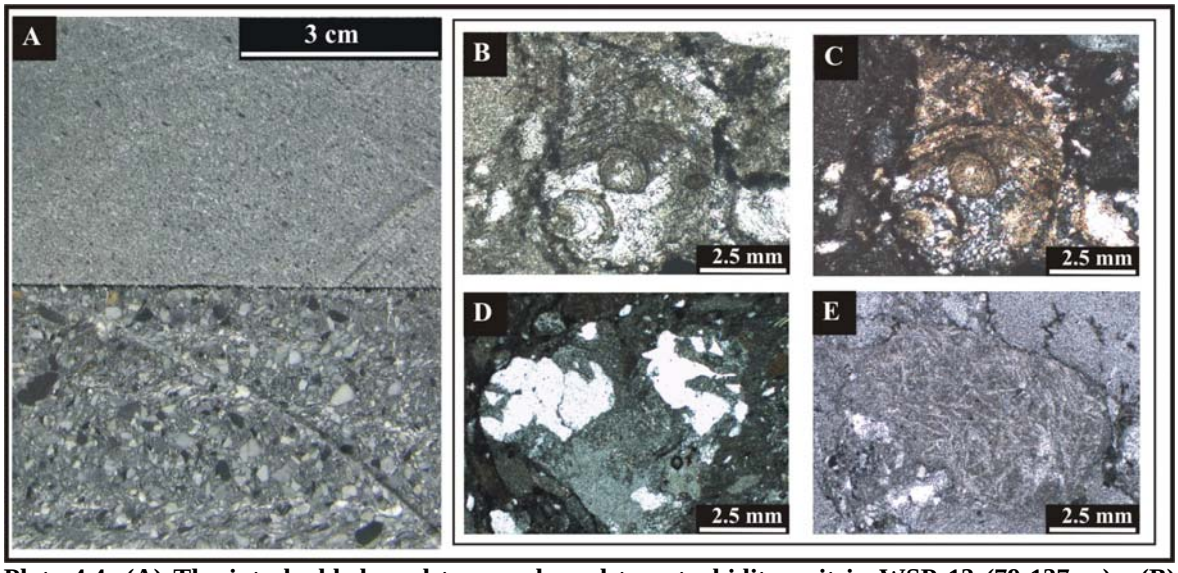

Plate 4.4: (A) The interbedded mudstone and sandstone turbidite unit in WSP 13 (79-137 m). (B) ?Fossiliferous limestone clast present at 79 m in WSP 13. (C) Crossed nicols of (B). (D) Granitoid clast with large quartz phenocrysts in a fine-grained feldspar groundmass (Crossed nicols) in WSP 13 at 79 m. (E) Possibly andesitic clast with interlocking feldspar crystals at 79 m in WSP 13.

Quartz, carbonate, $FeCO_3$ with pyrite form veinlets that can be parallel to S_o. The veins can also be deformed and folded. Siderite veins with pyrite are a later stage vein in WSP 12. Similar features are seen in the CVC of WSP 12. Minor brecciation of grey mudstone fragments with black mudstone infill can occur with quartz veins and sphalerite and galena. At 122.4 m in WSP 13, minor brecciation of mudstone with fine-grained sandstone infill is present and may be due to soft-sediment deformation. Irregular pods and lenses of sandstone are in the mudstone intervals and again, are possibly due to soft-sediment deformation. Numerous areas of broken core occur in this facies in both holes occur (E.g. WSP 13, 85.2–86.3 m, and 119–119.7 m, DCP 235, 28.3 m).

Interpretation of the Interbedded Mudstone and Sandstone Turbidite Facies

The fine–grained to medium–grained beds are sheet like and formed by turbidity currents in a deep subaqueous medial to distal setting (e.g. Cas & Wright, 1987; Pickering et al., 1989; Reading, 1986). The clay, silt and sand grains are suspended by fluid turbulence within the flow (Kano, 1996; Lowe, 1982). High concentration turbidity flows can form sandstone beds greater than 30 cm with reverse graded bases, massive middle sections and normal graded top beds (e.g. Cas & Wright, 1987; Lowe, 1982; Pickering et al., 1989; Walker, 1984). Low concentration flows could form beds less than 10 cm, with coarser

basal normally graded and planar beds, ripples and upper massive and laminated mud units (Cas & Wright, 1987; Lowe, 1982; Pickering et al., 1989; Walker 1984).

For the facies at White Spur, all these features are not present together or remain unseen; it is possible a flow of intermediate character formed the interbedded sequence. It may also be that the entire Bouma sequence is not present in the drillcore or outcrop due to several factors of the flow (e.g. distance travelled from the origin, fluctuating sediment load, the degree of flow expansion and flow velocity; Cas & Wright, 1987).

4.2.3 Felsic Facies Association

This facies association includes the feldspar-phyric dacite of the CVC directly below the contact with the White Spur Formation, and the feldspar-quartz-biotite-phyric rhyolite that lies above the contact.

4.2.3.1 Feldspar-Phyric Dacite Facies Association

The dacite facies occurs in the CVC footwall in drillhole WSP 10/10A from 460 m to the E.O.H (626 m). Coherent and clastic sections comprise the unit and vary in size. The unit is predominantly coherent.

The upper contact is unusual for the CVC-WSF contact. The contact contains 15 m of poorly sorted feldspar-phyric monomictic pumice breccia. Above the pumice breccia, the contact is irregular and contains feldspar-quartz-porphyritic pumice clasts in laminated grey siltstone. Mixing occurs between the pumice clasts and the grey siltstone over 5 m, with sphalerite and pyrite in the siltstone as disseminated grains and laminations. The lower contact of the dacite facies is not present in the available drillcore but the lower 5 m of the hole shows a perlitic coherent dacite interval.

The coherent dacite sections are feldspar-phyric and can be perlitic, pumiceous, flow banded, amygdaloidal or spherulitic (Plate 4.5). The plagioclase feldspars are 1–3 mm, white and prismatic (7-10%). Most crystals display a glomeroporphyritic texture and few crystals are isolated. The plagioclase can be unaltered or altered by sericite, chlorite and minor biotite and muscovite; a minority are altered to a bright apple green, possibly fuchsitic composition. Around 580 m, pale pink hematite dusted secondary feldspar

alteration appears in the primary feldspars. A granular texture in areas consists of smaller (1 mm) secondary feldspar that infills perlite kernels. This feldspar is subround to subangular and appears as a jigsaw-fit network.

Perlite occurs in the silicified groundmass in the coherent intervals. It is coarse (0.5–1 mm) and is chlorite altered and contains secondary feldspar infill. The fractures are evident in strongly silicified areas. The lower parts of the facies show preserved relic perlite in dark chlorite altered domains. Higher in the unit at 475 m, a perlite and pumice zone is present. The pumice is compacted, angular, and altered by black phyllosilicates. It can be visible in silicified bands and aligned at 468 m. The tube pumice dominates the upper coherent parts of the facies.

Sections of the coherent dacite are strongly amygdaloidal. The amygdales occur as zoned siliceous clusters with quartz, seconadry feldspar, carbonate or chlorite cores and either carbonate or sericitic rims. The amygdales can have associated pyrite or secondary feldspar haloes such as at 582 m. The amygdales are round and amoeboid with irregular but smooth edges. At 556 m, aligned fluidal lenticular amygdales occur and are oriented uphole.

Parts of the coherent dacite are locally flow banded, especially 555–584 m. It is pale coloured and aligned uphole. Flow banding within the coherent facies reveals more crystalline versus chlorite altered, possibly originally glassy areas. Fibrous spherulites are present in the coherent groundmass. The spherulites are 2 mm and appear as clusters. Rare 1-5 cm cream-brown fine-grained mafic clasts are scattered throughout the coherent dacite facies. There can be round to irregular. It is the only foreign lithic material within the dacite facies association.

The clastic dacite facies is minor and consists of monomictic breccias. The monomictic breccias have clasts of coherent feldspar-phyric dacite that are up to 64 mm. A few of the clastic breccia sections contain perlite, evident from the close network of small feldspar crystals and siliceous alteration. The perlite is highlighted by chlorite alteration of the fractures around the secondary feldspar crystals. The perlitic clasts could have been produced by quench fragmentation. A good example is at 507 m. No perlite is present in the other clastic breccia facies. Amygdaloidal clasts are evident in some of the breccia

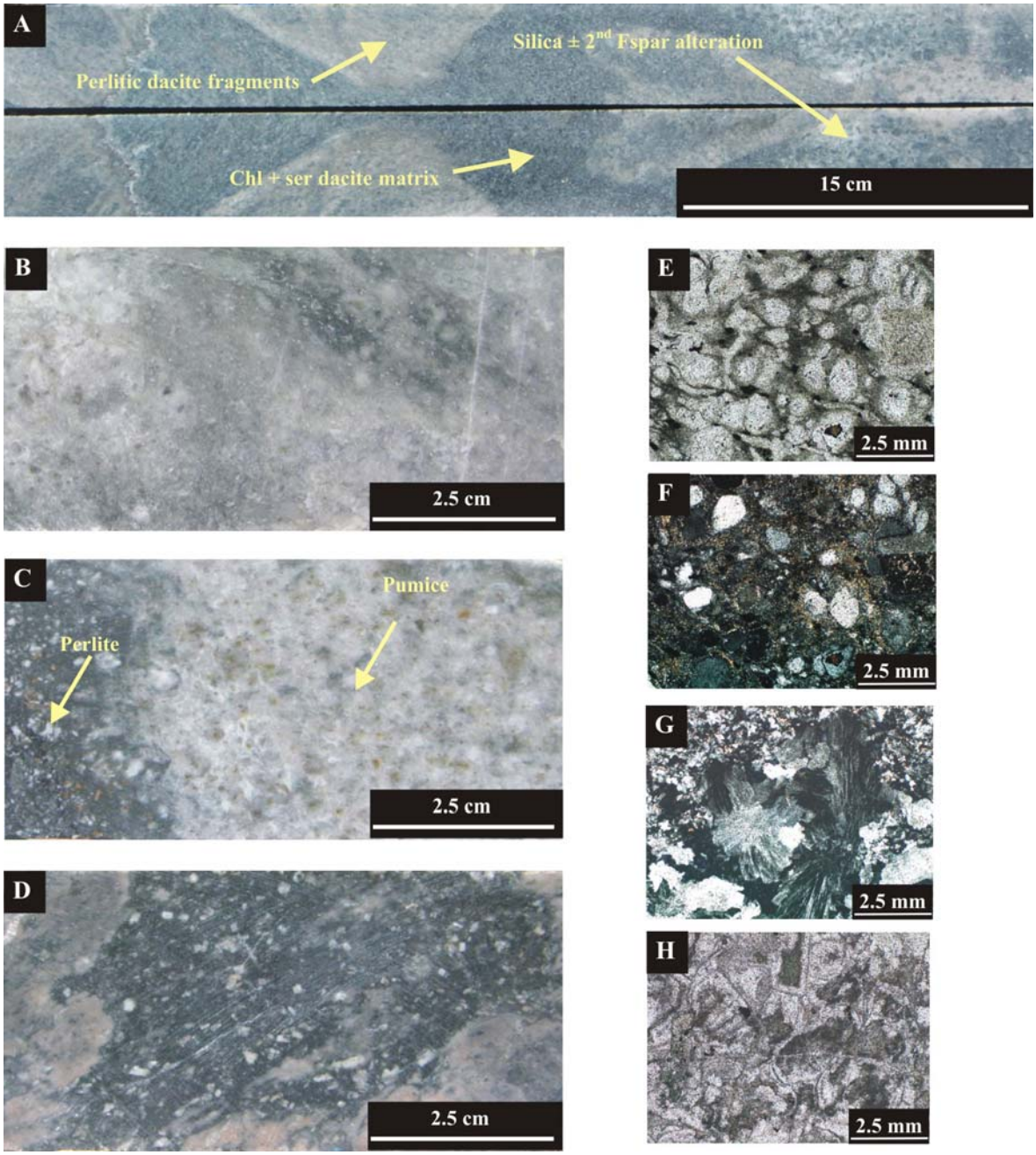

Plate 4.5: Feldspar-phyric dacite facies in WSP 10A. (A) Breccia facies at 29 m with perlitic dacitic fragments. (B) Pumice breccia at 457 m with disseminated pyrite. (C) Coherent perlitic (in chlorite domains) and pumiceous (in silicified domain) interval at 468 m (D) ?Pseudobreccia at 588 m produced by chlorite and secondary feldspar alteration. (E) Amygdales at 556 m with crossed nicols in (F) within coherent facies. (G) Spherulites in the coherent groundmass at 494 m (crossed nicols). (H) Perlite fractures at 583 m within a coherent interval.

units. Pumiceous and flow-banded clasts occur within breccia units that have no perlite. The tube pumice is randomly oriented and the flow bands end at clast boundaries. These clasts are very irregular in shape and vary in size. The pumiceous and flow-banded breccia is at 590 m.

The poorly sorted feldspar-phyric monomictic pumice breccia is 15 m thick and sits at 445-460 m above the coherent dacite facies. The contact between the two facies is gradational and extremely difficult to identify. It is noticed only by the appearance of clastic tube pumice and less perlitic domains. The tube pumice clasts are 1-2 mm but can reach 6 cm. The clasts have been altered by silica and secondary feldspar. The subrounded to subangular feldspars are 1-4 mm (10-15%) and can be white to bright apple green caused by alteration. Sulfides are evident (1%) as disseminated sphalerite grains. The facies has a grey to pale green cream mottled texture due to silica, sericite and carbonate alteration. In other areas, the white crystals are supported in a dark green to black phyllosilicate groundmass of sericite and chlorite with silica and carbonate. A classic example of pumice breccia is seen in TS 10A457.

$FeCO_3$, carbonate, chlorite and quartz veinlets are common throughout the facies. The alteration of the dacite is relatively uniform. Silicification is the dominant style for the majority of the facies and in parts a mottled texture along with chlorite. Below 580 m, silicification is replaced by selective but pervasive pink hematite dusted secondary feldspar and chlorite alteration that is distinctive of CVC footwall alteration. These alteration styles create pseudoclastic textures within the coherent dacite.

Interpretation of the Feldspar-Phyric Dacite Facies Association

The dacite facies association may be either a dome complex or cryptodome. It is likely that the facies is a dome complex possibly with numerous coherent lobes. This interpretation is suggested as no peperitic margins were observed and the facies association contains alternating clastic and coherent facies. A thick clastic interval is present at the top of the association. The associated pumice breccia is believed to be intruded by the coherent facies (Allen, 1998). In other unobserved areas of this study the ‘intrusion’ grades into pumice breccia. This pumice breccia may have been formed by the dome-like complex and has been resedimented over the coherent parts of the facies. The height of the

dome complex would be >180 m with a lateral extent of >500 m. The implications of this will be discussed in detail in following chapters.

4.2.3.2 Quartz-Feldspar-Biotite-Phyric Rhyolite

This unit occurs in WSP 12, DCP 235, WSP 10 and the Hall Rivulet Canal. It is 20 m thick in WSP 12, 17 m in DCP 235, at least 200 m in WSP 10 (Plate 4.6) and by the investigation from this research 70 m in the Hall Rivulet Canal. The occurrence in WSP 10 is underlain by the laminated pyritic black mudstone while the other occurrences lie at the CVC – White Spur Formation contact.

This facies is recognised by the appearance of quartz crystals, biotite abundance, textural change and intensity of silicification. The lower contact is faulted in DCP 235 and WSP 10, irregular but sharp in WSP 12 and obscured by silicification in the Hall Rivulet Canal.

The upper contact appears to be peperitic with pyritic black mudstone at ~ 229 m in WSP 12 and ~ 129 m in DCP 235. This is associated with intense brown silicic alteration close to the contact. The WSP 12 contact has unusual wispy pink secondary feldspar alteration with silicified haloes associated with it. The contact in the Hall Rivulet Canal is difficult to distinguish due to the exposure quality but certainly, the upper contact breccia contains perlitic rhyolite fragments. This peperite contact consists of the perlitic rhyolite fragments and fine-grained siliceous material. This facies in WSP 10 extends beyond the drillhole collar in WSP 10, and the upper contact was not observed. This facies contains dominantly clastic units and minor coherent units.

The porphyritic rhyolite contains phenocrysts of feldspar, quartz and biotite in a very fine silicified groundmass. The 1-3 mm isolated quartz crystals are clear and subround (7%) and contain numerous melt inclusions. The 1–4 mm feldspar phenocrysts are white and subround, lath or equant phenocrysts (5-7%). Some of the feldspar are lath plagioclase phenocrysts. These plagioclase phenocrysts can be glomeroporphyritic. Red and brown $FeCO_3$ grains, hematite-altered feldspar and apple green (?)fuchsitic-altered feldspar are also present. Carbonate can also alter the feldspar crystals. The biotite is 0.5-3 mm and is 3-5%.

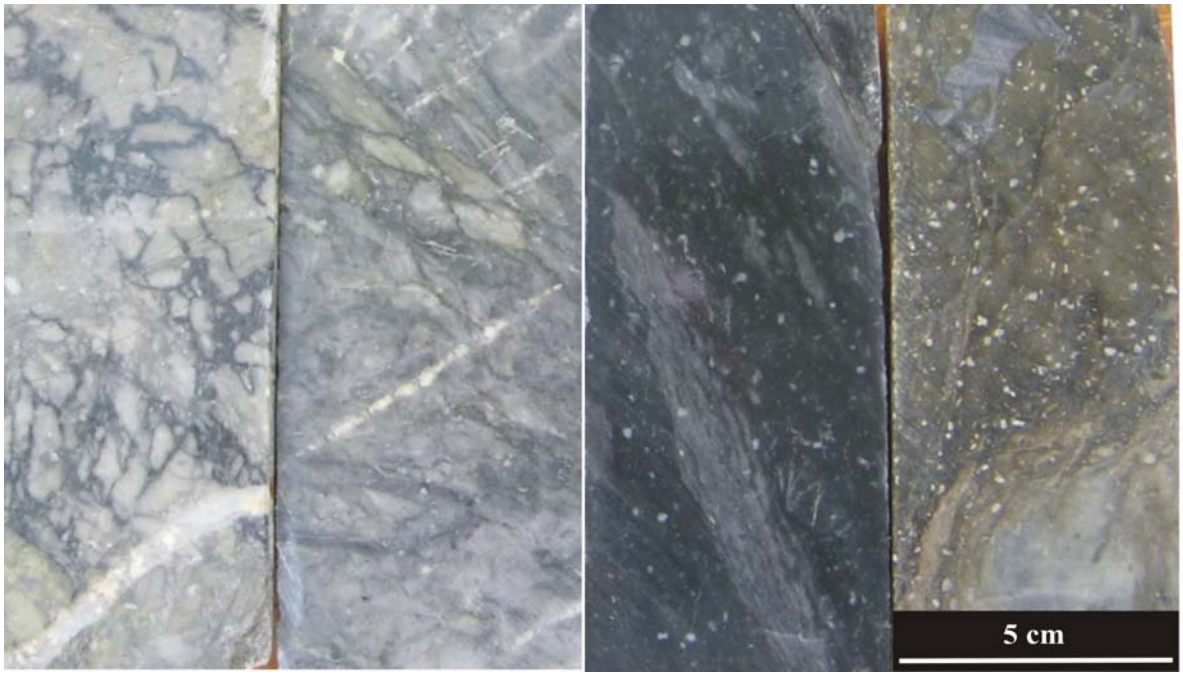

Plate 4.6: The rhyolite facies in WSP 10. From left to right (67-194 m) the facies is brecciated, coherent and flow-banded, possible pseudobreccia is evident in the far right sample (194 m).

The upper coherent facies contains feldspar-quartz porphyritic pumice in black chloritic groundmass is aligned uphole and is interconnected. Pumice is silicified and sericitic. Examples oocur at 55 m and 67.6 m. Lithic clasts of 1 mm black mudstone occur (5%) but rare and small 0.5–1 cm mudstone lithic clasts occur in WSP 12.

The coherent rhyolite has a slight green-grey and cream mottled alteration texture. Wispy phyllosilicate alteration is present along with red/brown $FeCO_3$ and hematite veinlets. Anastomosing carbonate veinlets occur in the groundmass. Brown leucoxene appears in the groundmass (1-3%) and as irregular patches in opaque phases. The groundmass consists of a 0.1 mm mircocrystalline mosaic. The silicified groundmass contains intense selectively carbonate alteration. Opaques phases cubic pyrite < 0.5 mm. Minor 1 mm epidote is present at 1%. Styolites of red, brown and green opaque material occur throughout the unit. The unit can be intensely pervasively sericitic and siliceous altered. The presence of perlite occurs. Perlite is outlined by fine-grained chlorite alteration. Flow-banding is represented by branching anastomosing and interconnected chlorite with silica infill. Three feldspar grain sizes occur in the facies; the first is up to 2 mm phenocrysts, the second is 0.2 – 0.5 mm secondary feldspar in perlite, and the last is the

<0.1 mm in the groundmass.

The clastic facies of WSP 10 spaced irregularly throughout the coherent facies (e.g. 63 m, 91.6 m, 157 m, and 181 m) contains blue-grey, silicified monomictic breccias. The angular fragments are coherent rhyolite up to 10 cm. The fragments consist of 15% feldspar, 7% quartz, pumice and minor sulfides. The white, subangular to subrounded feldspars can be 1–3 mm and can occur as laths. The quartz is grey to clear, subrounded to subangular, and is 1–3 mm. Pyrite occurs as <1 mm disseminated grains (1%). The compacted black pumice appears as thin, irregular, phyllosilicate-altered bands. Large carbonate grains infill the groundmass. The appearance seems porphyritic with the groundmass intensely altered to very fine silica and sericite (<0.1 m).

In places of WSP 10 (e.g. 63 m, 91.6 m, 157 m, and 181 m), the breccias have jigsaw-fit textures and extensive fracture networks. The fragments are silicified and some are sericitic. The clastic facies is jointed throughout and has minor chlorite, carbonate and quartz veins.

Blue-grey silicification is a dominant alteration style in the facies of WSP 10 and occurs in bands. A green brown alteration and grey and cream mottled alteration are the main styles. The flow-bands have grey silicified haloes and are highlighted by different alteration styles. The alteration style gives a pseudobreccia texture (e.g. 187 – 200 m). From 194 m to the end of the facies (200 m) abundant quartz veining occurs.

Interpretation of the Quartz-Feldspar-Biotite-Phyric Rhyolite

The facies is interpreted to be a syn-depositional sill. Evidence includes peperite margins at both lower and upper contacts. The clasts at these margins contain perlite, as seen in the Hall Rivulet Canal suggesting it to be quench brecciation. This breccia contains siliceous material enclosing the clasts similar to that above and below the body. The siliceous material may be thermally metamorphosed fine sediments (e.g. Hunns & McPhie, 1999). Metamorphism could have resulted from intrusion into wet unconsolidated sediments as a shallow level sill or cryptodome (Gifkins et al., 2002; Hunns & McPhie, 1999; Skilling et al., 2002). The brecciation seen in WSP 10 may be autobrecciation of coherent lava or lobes within the sill/cryptodome. The brecciation may have been consequent on continued

magma supply to the sill lobes, forcing expansion and brecciation of the coherent parts confined by the intruded wet sediments (c.f. Hunns & McPhie, 1999).

A summary of the main compositional and textural features of the facies is outlined in Table 4.1.

4.2.4 Stratigraphic Units

The complete stratigraphy of White Spur comprises the CVC at the base overlain by the White Spur Formation.

4.2.4.1 The CVC

The base of the known stratigraphy is the extensive pumice breccia of the CVC. This facies occurs in the footwall of all the outcrops and drillholes except one. The feldspar-phyric dacite facies association replaces the pumice breccia in WSP 10A. The relationship between the two is unclear at this time. The fine-grained Host Rock grades from the massive pumice breccia and sits at the top of the extensive unit. The Host Rock grades to black mudstone of the White Spur Formation.

4.2.4.2 The White Spur Formation

The base of the White Spur Formation consists of the black mudstone and sandstone turbidite lithofacies that can conformably or unconformably overlie the CVC Host Rock and pumice breccia respectively. The laminated pyritic black mudstone facies contains the quartz-feldspar-biotite-phyric rhyolite facies that occur at two separate stratigraphic positions. The confirmed quartz-feldspar-biotite-phyric rhyolite sill with peperitic margins occurs slightly above the White Spur Formation – CVC contact. The quartz-feldspar-biotite-phyric rhyolite of WSP 10 is believed to occur toward the top of the laminated pyritic black mudstone unit. The poorly bedded breccia facies of WSP 10 occurs within the laminated black pyritic mudstone facies.

The massive sulfide clast bearing mass-flow deposit overlies the laminated pyritic black mudstone unit. The crystal-rich mass-flow unit overlies the massive sulfide clast bearing mass-flow unit. Finally, the observable top of the White Spur stratigraphy contains the

interbedded mudstone and sandstone turbidite unit that overlies the crystal-rich mass-flow deposit.

4.3 Summary

Composition, lithology, texture, contact relationships and depositional processes distinguish the main volcano-sedimentary facies in the White Spur stratigraphy. The graded volcaniclastic facies includes the quartz-feldspar-phyric mass-flow facies of the White Spur Formation and the underlying feldspar-phyric pumice breccia and associated feldspar-phyric pumiceous stratified sandstone of the CVC. The sedimentary facies associations include the laminated pyritic black mudstone that contains sandstone turbidites and the upper interbedded mudstone and sandstone turbidite facies. Both these facies occur in the White Spur Formation. The feldspar-phyric dacite facies association of the CVC and the quartz-feldspar-biotite-phyric rhyolite of the White Spur Formation comprise the felsic facies association subdivision.

Chapter 5 Correlation of the White Spur Stratigraphy

5.1 Introduction

The separate facies of the White Spur stratigraphy are decribed in detail in chapter 4. In this chapter, correlations and the volcanic facies architecture of the White Spur area are discussed.

The correlations were made with the production of fence diagrams based on the stratigraphic data obtained from the five diamond drillholes and three mapping areas examined for this project. These data were combined with the fence diagram of the White Spur stratigraphy produced by Allen (1997 unpub.) and updated. Due to the scale of the research, the fence diagrams had to be divided into southern (Figure 5.1) and northern (Figure 5.2) areas.

The original drill logs of this study can be viewed in appendix 2. The fence diagram created by Allen (1997 unpub.) appears in appendix 3.

5.2 Correlation of the CVC

5.2.1 Feldspar-Phyric Pumice Breccia

This facies is simple to correlate due to the extensive, distinctive and uniform nature. It extends from the Anneliese 1 drillhole in the south of the area to beyond the study area to the Hercules deposit to the north. The pumice breccia is uniform in appearance with the maximum thickness seen in Anneliese 1 being ~150 m as the drillhole intersects a fault, probably the North Henty Fault. Interestingly, in Anneliese 1 massive pyrite occurs 100 m below the White Spur Formation – CVC in the pumice breccia. Erosion of the CVC, possibly by shallow marine processes, is thought to have produced sub-basins (Allen, 1997 unpub.).

The Host Rock is simple to recognise, yet difficult to correlate. Local erosion of the CVC pumice breccia seems to have removed these important rocks from the White Spur area.

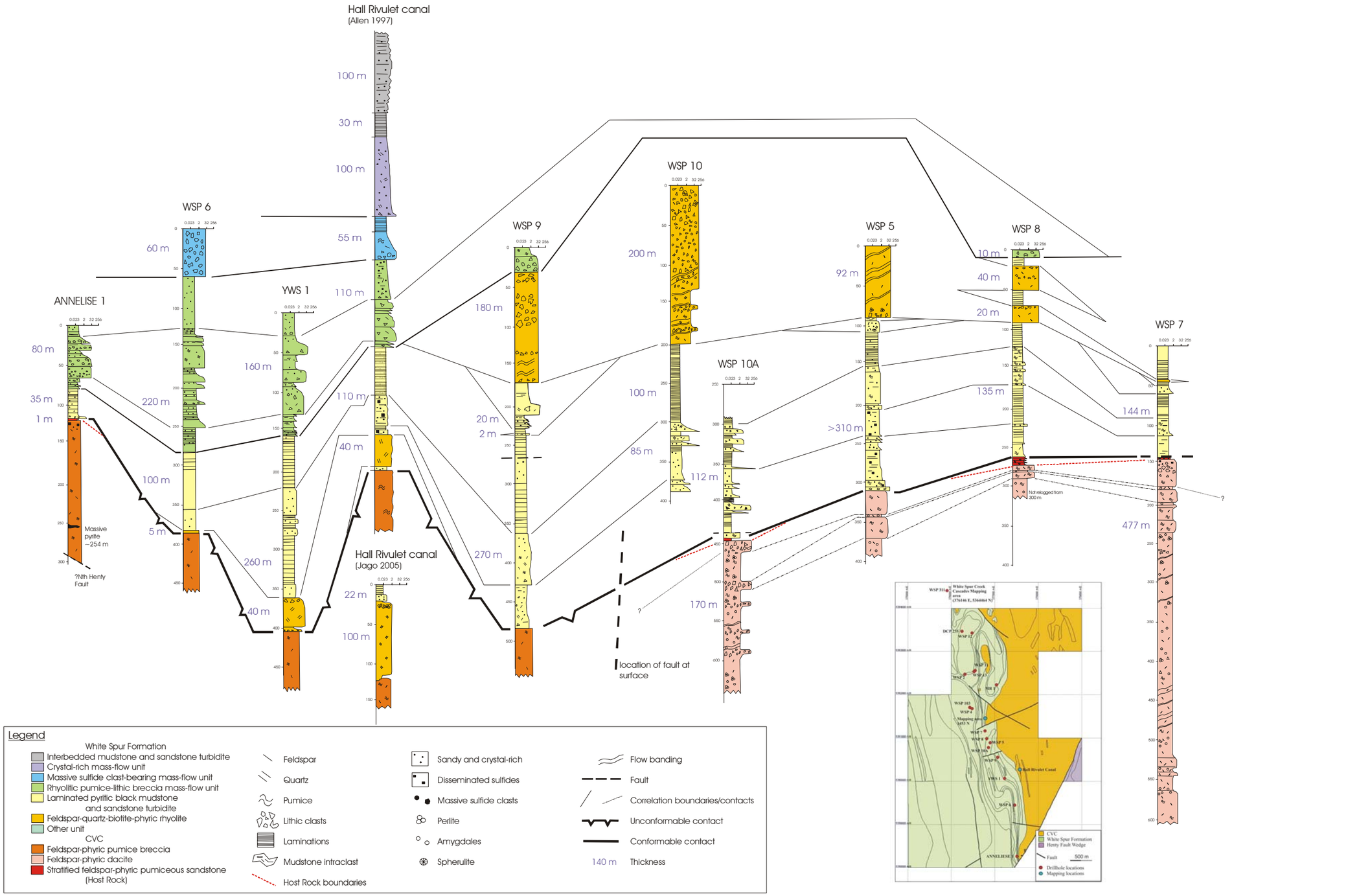

Figure 5.1: Fence diagram showing the correlations of the major lithofacies of the White Spur Stratigraphy of the southern area of the White Spur EL. South to north is indicated from left to right.

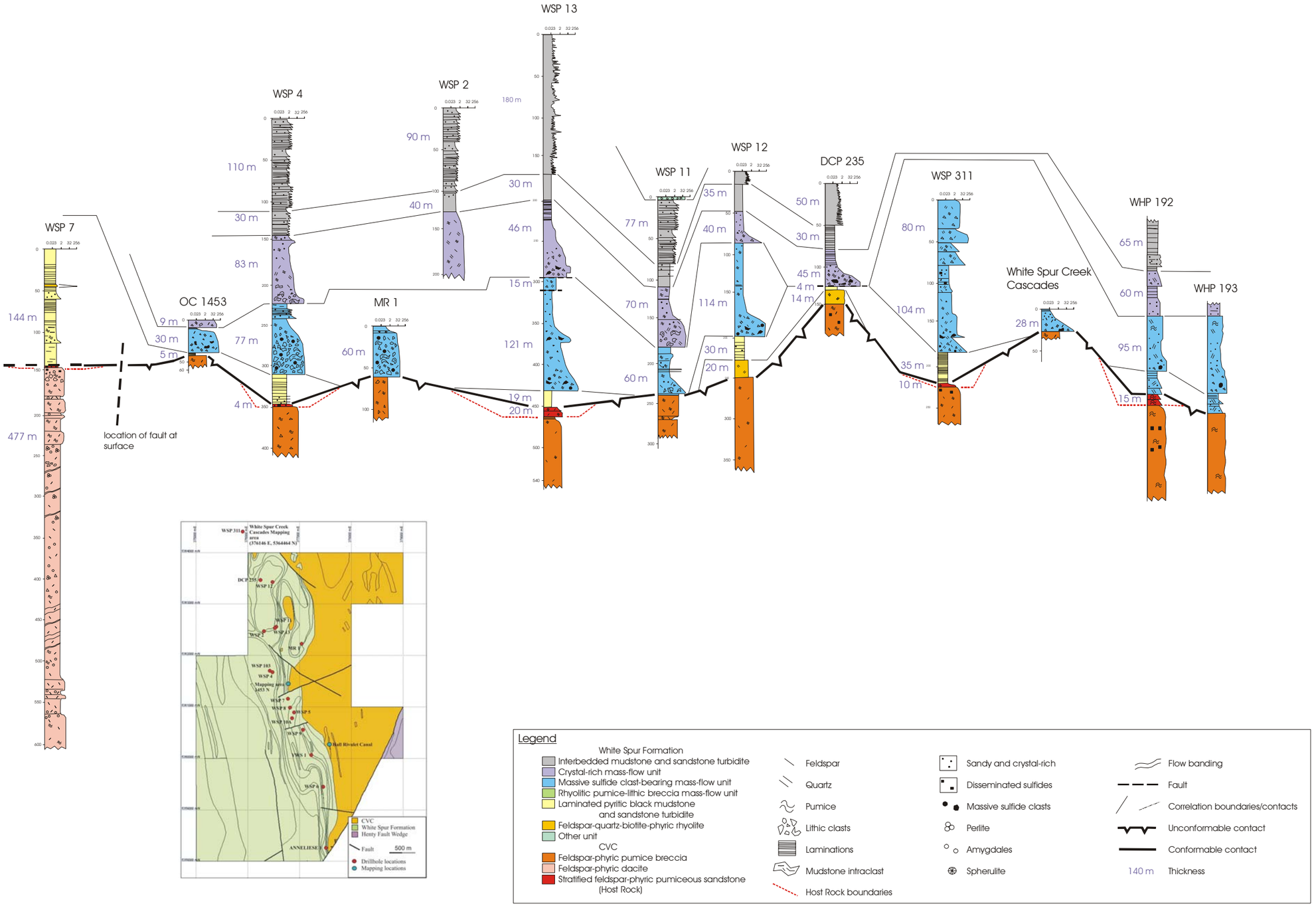

Figure 5.2: Fence diagram showing the correlations of the major lithofacies of the White Spur Stratigraphy of the northern area of the White Spur EL. South to north is indicated from left to right.

In addition, faulted contacts between the White Spur Formation and the CVC seem to have contributed to the disappearance of the Host Rock from areas of the White Spur stratigraphy (WSP 7).

Unexpectedly, the Host Rock is intact in several areas discovered by this study. A minor 1 m interval is interpretated in Anneliese 1. No other occurrence of the Host Rock is evident in the southern area of the White Spur EL. WSP 7 has a 2 m interval of brecciated stratified sandstone (depth: ~145 m) caused by a post-depositional fault that removed the unit. In the northern area, the Host Rock occurs in drillholes WSP 4, WSP 13 and WSP 311. The occurrence in WSP 4 is 4 m thick and contains 2% disseminated pyrite, pyrrhotite and sphalerite. In WSP 13, the Host Rock is significant at a thickness of 20 m of stratified feldspar-phyric pumice sandstone. Disseminated sphalerite and pyrite occur at 3%. A graded volcanic sandstone bed of 10 m thickness occurs in WSP 311 and represents the Host Rock.

Importantly, the two drillholes adjacent to mapping area 1453 N contain Host Rock. It was inferred from mapping for construction of the fence diagram that the contact between the White Spur Formation and CVC was disconformable. This contact is quite difficult to distinguish due to lack of crucial outcrop. The host rock may exist continuously from WSP 7 to WSP 4 through mapping area 1453 N. This interpretation warrants further study.

5.2.2 Feldspar-Phyric Dacite

An isolated syn-volcanic dacite complex is present in the immediate CVC footwall within the central area of the EL. This is an unusual occurrence in the CVC in the White Spur area and can be correlated between drillholes with ease. The dacite appears in drillholes WSP 10/10A, WSP 5, WSP 8 and WSP 7. The base of the dacite is not visible in any drillhole. The thickness is at least 170 m in WSP 10A, 75 m in WSP 5, 50 m in WSP 8 and 477 m in WSP 7. The lateral extent is at least 500 m between WSP 7 and WSP 10. Correlation within the facies is possible between the alternating coherent and clastic sections. The upper unit immediately below the White Spur Formation contact includes a monomictic pumice breccia interval and a underlying perlitic and/or amygdaloidal,

pumiceous coherent interval, this is followed by repetition of these facies.

5.3 Correlation of units within the White Spur Formation

5.3.1 Laminated Pyritic Black Mudstone

This is the first and lowest unit of the White Spur Formation and is evident throughout most of the area. It is prominent in the southern end of the study area from Anneliese 1 to WSP 7 ranging from 35-270 m. Anneliese 1 has 35 m of black mudstone that expands to 100 m in WSP 6. The thickness of the mudstone and turbidites in YWS 1 and Hall Rivulet Canal is 260 and 110 m respectively. The greatest thickness of this facies is in WSP 9 (270 m) comprising black mudstone, siltstone and sandstone turbidite beds. WSP 10/10A contains turbidite breccia beds within the mudstone and can be correlated with the poorly bedded coarse sandstone beds in WSP 9 and WSP 5. The package is 212 m thick in WSP 10/10A, 200 m in WSP 5, 250 m in WSP 8 and at least 150 m in WSP 7.

To the north, at the mapping area 1453 N, the mudstone is 5 m thick and the nature of the contact is unknown. Adjacent to this hole is WSP 4 that contains 40 m of black mudstone overlying host rock. The package disappears and is not represented in the nearby MR 1 drillhole. In WSP 13, the package reappears 19 m thick and lenses out and absent in WSP 11. WSP 12, DCP 235 and WSP 311 contain the package 30, 4 and 35 m respectively. The thin nature in DCP 235 is due to a major normal fault. The package does not occur at the White Spur Creek Cascades.

5.3.2 Quartz-Feldspar-Biotite-Phyric Rhyolite

The rhyolite intrusion is irregular in occurrence and distribution. The rhyolite occurs at two stratigraphic positions at the upper and lower contacts of the black mudstone package. The lower rhyolite occurs in WSP 6, YWS 1, Hall Rivulet Canal, WSP 12 and DCP 235. The thickness ranges from 5 – 40 m. North from Hall Rivulet Canal to WSP 9, the rhyolite appears higher in the stratigraphy. It remains at this position from WSP 9 to WSP 7 through WSP 10, WSP 5 and WSP 8, ranging from 2 m to 200 m thick, averaging ~100 m. At WSP 8, the rhyolite is separated into two bodies 40 and 20 m thick. The lower of these bodies extends to WSP 7 as a 2-3 m unit.

The rhyolite is absent from the majority of the northern area, apart from WSP 12 and DCP 235 20 and 14 m thick respectively. It occurs at the contact between the White Spur Formation and the CVC.

The rhyolite either may be the same intrusion or two separate intrusions. If the rhyolite occurs as one intrusion, the correlations between Hall Rivulet Canal and WSP 9 are difficult to support this. This interpretation will be discussed later.

5.3.3 The White Spur Formation Volcaniclastic Mass-flow Units

The correlation of the mass-flow units are primarily based on the presence of certain clast types along with the crystal content and larger scale features including lithology, composition and contact relationships. Three mass-flow units are identified at White Spur. The rhyolitic pumice-lithic breccia mass flow unit (described below), overlies the laminated pyritic black mudstone and is considered the lowest mass-flow unit in the White Spur stratigraphy. The massive sulfide clast bearing mass-flow unit is the second mass-flow unit of the stratigraphy and overlies the rhyolitic pumice-lithic breccia mass-flow facies. The third mass-flow unit present in the stratigraphy if the crystal-rich mass-flow unit that overlies the massive sulfide clast bearing mass-flow unit.

5.3.3.1 Rhyolitic Pumice-Lithic Breccia Mass-Flow Unit

This is the second unit of the White Spur Formation and is the lowest mass-flow unit in the stratigraphy. The rhyolitic pumice-lithic breccia mass-flow unit occurs in the southern area and was not observed in drillcore or mapping during the project. Allen (1997 unpub.) described the facies has being a rhyolitic pumice-lithic breccia with <4% quartz and weakly porphyritic rhyolite clasts and black mudstone clasts supported in a black mud matrix. This unit consists of numerous graded beds from breccia base to siltstone top.

In Anneliese 1, 60 m of the unit is exposed. The unit comprises a lower stratified and graded part 40 m thick, overlain by a graded part at least 20 m thick. The unit extends to WSP 6 and expand to 220 m. This thickness is at least 160 m in YWS 1 and decreases to 110 m at Hall Rivulet Canal. The unit is present at the top 25 m of WSP 9 as the hole was collared in this unit. The unit reappears at WSP 8 with only 10 m occurring at the top of

the hole. This is the last exposure present in the White Spur area, as no northern representation exists.

5.3.3.2 Massive Sulfide Clast Bearing Mass-Flow Unit

This is the third unit of the White Spur Formation and is the second mass-flow unit, the feldspar-quartz-phyric pumice breccia. This deposit is predominant in the northern area and there are only two occurrences in the southern part of the EL in WSP 6 and Hall Rivulet Canal.

A pebble-cobble breccia is present in WSP 6 and is at least 60 m thick at the top of the hole. At Hall Rivulet Canal, a massive and graded 35 m thick mass-flow deposit with a breccia base and siltstone top represents the unit. A 20 m mudstone bed overlies this. The unit is not observed until mapping area 1453 N (30 m thick). The exposure is predominantly cobble breccia that grades to siltstone only in the upper 3 m. In WSP 4, the unit is 77 m thick and predominantly cobble breccia that grades to siltstone close to the top of the unit. The mass-flow deposit of MR 1 is 75 m thick and grades to siltstone. This occurrence is significant due to the abundance of the characteristic massive sulfide clasts.

WSP 13 shows a mass-flow deposit 121 m thick that grades to siltstone. A 15 m thick, fault-bound sandstone interval of the same facies overlies the main unit. The unit is represented by 60 m and 117 m in WSP 11 and WSP 12, respectively. The unit does not occur in DCP 235 and is possibly due to a large fault present that has removed a significant proportion of the stratigraphy. The unit occurrence in WSP 311 is very unusual. The normally graded unit seen throughout the area is present 104 m thick. At least an additional 80 m thick of poorly bedded breccia overlies the main unit. The unit at the White Spur Creek Cascades is 28 m thick and grades from cobble breccia to siltstone. The unit can be traced further north to the Hercules area.

5.3.3.3 Crystal-Rich Mass-Flow Unit

The third mass-flow unit is the fourth unit of the White Spur Formation and is feldspar-quartz crystal-rich sandstone. The mass-flow unit is mainly exposed in the northern area with one occurrence at Hall Rivulet Canal to the south.

At Hall Rivulet Canal, the unit is 100 m thick and consists of a massive and graded mass-flow deposit with a minor breccia base that grades to sandstone. To the north, in WSP 4 the lithology is similar but is 83 m thick. The unit is similar in WSP 2 and WSP 13 but the upper portion is dominated by laminated siltstone. WSP 11 contains a 70 m breccia and sandstone unit that is almost half the size (40 m) in WSP 12 and grades from pebble-cobble breccia to siltstone that is similar in DCP 235. The DCP 235 exposure is the last occurrence in the White Spur area but can be tracked to Hercules.

At South White Spur (close to WSP 11, WSP 12 and DCP 235), the unit consists of two distinct parts: a lower stratified unit with feldspar >> quartz and 15–20% crystals 45 m thick; and an upper division of graded beds about 45 m thick with feldspar equal to quartz, and 15–20% crystals.

5.3.4 Interbedded Mudstone and Sandstone Turbidite

The fifth unit is a thick interbedded mudstone and sandstone turbidite package. It sits at the top of the stratigraphy mainly in the northern area, with one occurrence in the southern area at Hall Rivulet Canal.

The package is seemingly uniform throughout the entire area, with a lower 30-40 m mudstone unit and an upper 77-100 m thick interbedded turbidite unit. This unit does vary beyond the White Spur area into the Hercules area. Interesting, a higher unit overlies the interbedded mudstone and sandstone turbidite sequence at the top of WSP 11. The exposure is only 5 m thick and appear to be cobble breccia.

5.4 Facies Architecture of the White Spur Area

5.4.1 Formation and Emplacement of the CVC at White Spur

5.4.1.1 Feldspar-Phyric Pumice Breccia

The pumice breccia units in the CVC were transported and deposited by water-supported high concentration turbidity currents and water settled fallout (Allen, 1997 unpub.; Allen & Cas, 1990; Gifkins, 2001 unpub.). The finer-grained Host Rock was partly deposited by syn-eruptive water-settling and lower energy turbidity currents (Gifkins, 2001 unpub.).

Some of the deposition was attributed to post-eruptive processes and reworking (Allen, 1991 unpub.).

Also, upon correlation of the CVC stratigraphy, sub-basins are observed. From this study, the laminated pyritic black mudstone and Host Rock occurrences are observed to be associated with these basins, and are important structural features in exploration.

A large sub-basin is evident in the entire southern area. It extends over 3 km from Anneliese 1 to WSP 7 and is 35->300 m thick. Smaller basins (4-35 m thick) that contain intact Host Rock occur in the northern area. The lateral extensions are smaller (~75 m) but several Host Rock occurrences are evident.

The absence of Host Rock in numerous areas can be explained by several alternative interpretations.

- Syn-depositional faults may have raised the unconsolidated pumiceous deposits of the CVC to shallower settings, promoting erosion and locally removing the Host Rock facies.

- A mass-flow gravity current may have scoured down into underlying unconsolidated CVC, locally removing the Host Rock facies.

- The Host Rock may have never been deposited to begin with.

Allen and Cas (1990) proposed that the Rosebery-Hercules massive sulfide district formed in a submarine pyroclastic caldera. The formation of the sub-basins could have been influenced by faults generated by collapse and differential movement of blocks within a caldera (Allen, 1997; unpub.). Although Host Rock is not present in all the exposures, it remains possible that Host Rocks may lie down dip or along strike of the basins or of the known occurrences.

The formation of the pumice breccia was contemporaneous with a large-scale explosive eruption. The Kershaw Pumice Formation volume is >24 km^3 and its eruption probably led to synchronous caldera subsidence (Gifkins, 2001 unpub.). Movement on faults associated with piecemeal caldera collapse (Allen, 1991 unpub.) may have produced topographic variations in the unconsolidated pumice breccia. Higher blocks would have been eroded, allowing reworked deposits to pond in the lower topographic sub-basins. The Host Rock would be preferentially preserved in the sub-basins.

5.4.1.2 Feldspar-Phyric Dacite

The occurrence of the dacite at the top of the CVC can be explained by two alternative interpretations. (1) The dacite was emplaced either on the seafloor or sub-seafloor

following the caldera eruption (Allen, 1997; Gifkins; 2001 unpub.). (2) The dacite was emplaced lower in the CVC stratigraphy and then was displaced by syn-depositional faulting. This interpretation is supported by the presence of two faults within the CVC. These faults lie just north of WSP 7 and south of WSP 10, which coincides with the lateral extent of the dacite. The faults may have occurred in the time gap between the end of CVC deposition and beginning of the White Spur Formation emplacement.

It is interpreted that the upper and lower occurrences are separate intrusions. The higher rhyolite is confined laterally compared to the lower rhyolite but is thicker and shows a diverse range of textures. The lower rhyolite is established at the White Spur Formation – CVC contact and is laterally extensive but thinner.

5.4.2 Formation and Emplacement of the White Spur Formation

The White Spur Formation was formed adjacent to a rhyolitic volcanic centre in a below-wave-base setting (Gifkins, 2001 unpub.).

5.4.2.1 Laminated Pyritic Black Mudstone

This facies is governed by the sub-basins in the CVC pumice breccia. This relationship was first recognised by Allen (1997 unpub.) with the construction of the original White Spur stratigraphy fence diagram. As the first and lowest unit of the White Spur Formation, the laminated pyritic black mudstone and associated stratified feldspar-crystal-rich sandstone would be affected more by the sub-basins and would allow greater accumulation of material. The greatest thickness in the southern area reflects the presence of sub-basins. The sub-basin development may be due to shallow marine erosion, mass-flow processes or syn-depositional faulting. Because the mudstone locally overlies the Host Rock conformably in areas, development of the sub-basins by syn-depositional faulting is favoured.

Suspension processes formed the black mudstone. Low-energy turbidity currents introduced coarser volcanic sediment into the sub-basins, producing the sandstone laminae and breccia beds observed within the predominantly black mudstone lithofacies.

5.4.2.2 Quartz-Feldspar-Biotite-Phyric Rhyolite

The change of the stratigraphic position of this unit may be due to two factors. The first is that the two rhyolite intervals are separate bodies. The other possibility is that one rhyolite that has intruded several mechanically weak locations in the stratigraphy, in this case, the contacts between massive units and the more brittle mudstone. The rhyolite facies is focused into the CVC sub-basins.

Based on the fence diagram, it is interpreted that two rhyolite sills are present. The surrounding laminated pyritic black mudstone units correlate well between Hall Rivulet Canal and WSP 9. The form and textures of the bodies in this area are diverse. The higher rhyolite is confined laterally and thicker (20->200 m). The lower rhyolite is established at the White Spur Formation – CVC contact and is laterally extensive but thinner (5-40 m).

5.4.2.2 Mass-flow Deposits

The mass-flow deposits provide the best framework for correlation as pumiceous volcaniclastic facies are produced in large volumes, erupted infrequently, emplaced rapidly, and are widely distributed (McPhie & Allen, 1992).

Rhyolitic pumice-lithic breccia mass-flow deposit

The greater thickness in the southern area is due to the presence of sub-basins. This mass-flow would have travelled across such basins that would have contained the lower laminated pyritic black mudstone.

The unit only occurs in the southern end of the area, possibly due to topographic obstacles channelling the currents in the area. Such flows possibly eroded the sub-basins further, as the flow strength would be greater.

The massive sulfide bearing mass-flow deposit

The recognition of the massive sulfide bearing mass-flow is crucial in the search for VHMS style mineralisation in the White Spur area. The extensive nature of this unit suggests that it was not affected by the CVC sub-basins as the basins were already full. If indeed the current direction was from the south then the more stratified units in the northern area may be the finer grained and less dense material of the remaining waning

currents. The coarser particles were deposited in the southern regions, due to the flow being closer to the origin.

The absence of the massive sulfide bearing mass-flow in DCP 235 and the stacking in WSP 311 may be due to a structural control. A fault is present in DCP 235 at the base of the third mass-flow deposit. This fault may have removed the sulfide clast bearing mass-flow from the DCP 235 area and moved to towards the WSP 311 area. However, no major structure was evident in WSP 311.

The crystal-rich mass-flow deposit

There are marked changes in the bedforms and sedimentary textures from south to north. The more massive beds to the south show the beginning of the flow with overlying stratified top units of the current to the north. Also, the sorting of crystals around the DCP 235 area may highlight sorting features and flow dynamics.

5.4.2.3 Interbedded Mudstone and Sandstone Turbidite

This unit is laterally extensive and has constant thickness, suggesting that sedimentation was uniform throughout the White Spur area and was unhindered by palaeotopography caused by sub-basins and graben structures.

5.4.3 Synthesis

The CVC pumice breccia was deposited in a marine setting after an explosive caldera eruption. Caldera subsidence occurred by syn-depositional faulting creating elevation differences in the unconsolidated pumice breccia. The deposition of the feldspar-phyric sandstone and siltstone (Host Rock) followed subsidence and was deposited differentially on the fault blocks. Local gravity currents caused erosion of the higher fault blocks and redeposited the pumiceous material (including Host Rock) into the sub-basins. A post-caldera dacitic cryptodome intruded the pumice breccia facies. The black mudstone formed in the sub-basins by suspension processes and low energy turbidity currents. Quartz-phyric mass-flow gravity currents deposited the White Spur Formation. Sub-seafloor replacement created massive sulfide lenses (Gifkins, 2001 unpub.). The sub-basins were filled. Subsequent water-supported mass-flow gravity currents were

unhindered by the sub-basins, as the topographic variation was relatively low. Turbidity currents deposited an extensive and uniform interbedded mudstone and sandstone sequence.

5.5 Summary

Lithological similarities and stratigraphic positions are used to correlate the units of the White Spur area. The CVC pumice breccia is extensive throughout the area with local dacite facies present. The Host Rocks do occur in several areas. The laminated pyritic black mudstone and rhyolitic pumice-lithic breccia mass-flow deposit are common in the southern end of the White Spur area and are restricted to sub-basins within the CVC. The other mass-flow deposits are laterally extensive over the White Spur EL. The interbedded mudstone and sandstone turbidite package remains uniform in thickness and is laterally widespread.

Chapter 6 Exploration and Mineralisation Potential

6.1 Introduction

The White Spur area is geologically interesting for the exploration potential of the area. The contact between the WSF and CVC is interpreted to be highly prospective for VHMS mineralisation as the Rosebery and Hercules deposits lie at that stratigraphic position.

6.2 The Stratigraphy of Rosebery and Hercules

Chapter 3 describes the Rosebery-Hercules Host Sequence in detail. The sequence from the bottom of the stratigraphy includes the Footwall Pyroclastics, the Host Rock, Black Mudstone and the Hangingwall Volcaniclastics. Tables 6.1 and 6.2 summarise the Rosebery-Hercules Host Sequence at the Rosebery and Hercules deposits respectively.

Table 6.1: The stratigraphic units and facies east of the Rosebery Fault in the Rosebery area. The stratigraphy is represented from bottom to top of the table.

Rosebery Stratigraphy	Constituent Facies	
White Spur Formation	Subaqueous quartz-feldspar-phyric mass-flow units (Hangingwall Volcaniclastics)	50-200 m
	Black mudstone (Black Slate)	0-30 m
CVC		
Hercules Pumice Formation	Tuffaceous shale (Host Rock)	35 m
	Feldspar-phyric pumice breccia (Footwall Pyroclastics)	>300 m

The stratigraphy between Rosebery and Hercules is similar in facies and facies thickness. Both deposits include older CVC in the hangingwall stratigraphy caused by thrust faulting of the CVC (Allen, 1991 unpub.; Gifkins, 2001 unpub.). The stratigraphy observed at White Spur is similar to that of Rosebery and Hercules. The White Spur stratigraphy is summarised in Table 6.3.

Table 6.2: The stratigraphic units and facies of the Hercules area. The stratigraphy is represented from bottom to top of the table.

Hercules Stratigraphy	Constituent Facies	
White Spur Formation	Subaqueous quartz-feldspar-phyric mass-flow units	~50 m
	(Hangingwall Volcaniclastics)	
	Black mudstone (Black Slate)	~50 m
CVC		
Hercules Pumice Formation	Fine-grained pumice sandstone (Host Rock)	? m
	Feldspar-phyric pumice breccia	>500 m
	(Footwall Pyroclastics)	

Table 6.3: The stratigraphic units and facies of the White Spur area. The stratigraphy is represented from bottom to top of the table.

White Spur Stratigraphy	Constituent Facies	
White Spur Formation		
Interbedded turbidite unit	Interbedded mudstone and sandstone turbidite units	35-130 m
Mass-flow deposits	Crystal-rich mass-flow units	9-100 m
	Massive sulfide clast bearing mass-flow units	30-184 m
	Rhyolitic pumice-lithic breccia mass-flow units	10-220 m
Black Mudstone	Black mudstone	5-270 m
	Quartz-feldspar-biotite rhyolite	2-200 m
CVC		
Host Rock	Fine-grained sandstone top to pumice breccia	1-20 m
Footwall	Feldspar-phyric pumice breccia	>150 m
	Feldspar-phyric dacite	>477 m

The Hangingwall Volcaniclastics are quite similar to the White Spur Formation. As discussed in chapter 3, correlation between the two hangingwall sequences from Rosebery to White Spur is possible.

6.3 Mineralisation in the White Spur Area

Sulfide mineralisation occurs in outcrops at White Spur (5364710 N, 375560 E), White Spur Creek (5367770 N, 375480 E) and south of Conliffe Creek along a fault (Lees, 1987 unpub.). The fault marked by quartz veins with sporadic galena (Lees, 1987 unpub.). At Hamilton's Workings south of Williamsford, the stoped narrow quartz veins were probably auriferous (Lees, 1987 unpub.). This style of mineralisation is unresolved due to the ratios between the metal contents; Pb>>Zn and Ag is high, with no corresponding Au (Lees, 1987 unpub.).

The sulfide clasts in the massive sulfide clast bearing mass-flow unit are of great significance. Indication of the flow direction of the mass-flow could assist in the exploration for the source massive sulfide deposits. Interpretations from bedforms of the other two mass-flow deposits suggest that the flow direction and provenance was to the south (Allen, 1991 unpub.; Vicary, 1998 unpub.). The sulfide clasts were incorporated by a mass-flow gravity current through the erosion of a massive sulfide deposit (Vicary, 1998 unpub.). Clasts of this nature occur close (<1 km) to the Rosebery and Hercules deposits within erosive mass-flow units of the Rosebery-Hercules Hangingwall Volcaniclastics (Allen, 1991 unpub.).

Anneliese 1 contains massive sulfide lenses within intensely sericitic CVC pumice breccia about 100 m below from the White Spur Formation contact (Vicary, 1998 unpub.). It is in close proximity to the North Henty Fault that may have been a fluid conduit during mineralisation (Vicary, 1998 unpub.). To the south, a sericite-pyrite alteration zone is situated in the upper CVC (Vicary, 1998 unpub.). WSP 5 intersected this zone and assay results show 17 m at 0.77% Zn and 0.4% Pb (Vicary, 1998 unpub.).

The mineralisation in WSP 5 is replacement style disseminated pyrite-sphalerite-galena and follows the contact between the CVC footwall comprising of the dacite facies and the overlying stratified crystal-rich sandstone and grey siltstone Host Rock (Allen, 1998 unpub.). The adjacent WSP 10 and WSP 8 are less altered and mineralised. The grey siltstone above the dacite in WSP 10A contains laminations of sphalerite (3%) with large porphyritic pumice clasts. The sphalerite has a wispy appearance and reveals the

replacement of pumice by sulfides.

6.4 Implications of New Stratigraphic Correlations for Mineralisation in the White Spur Area

This section will suggest favourable positions for exploration based on geological features including the presence of the host rock, significant mineralisation, and structural controls.

The sandstone-siltstone top of the pumice breccias is present in several areas of the White Spur EL made obvious by the fence diagrams. The exposures Host Rock is exposed as < 5 m in Anneliese 1, WSP 10, WSP 5 and WSP 7.

The southern area contains one large sub-basin in the CVC from 35-270 m thick. The sub-basins are important as the Rosebery and Hercules massive sulfide deposits occur in these sub-basins. Recognition of these sub-basins and defining the larger basins can potentially help in exploration of VHMS ore deposits.

The black mudstone that characterises the basin is a part of the host stratigraphy. Therefore, the entire basin is an exploration target. The Host Rock could lie along strike or down dip within this basin. It seems unnecessary to focus exploration mainly within the thickest parts of the basin as the Host Rock distribution is unaffected by this factor. The simplest solution would be to search the areas where growth faults are expressed at the surface. These locations are north of WSP 7, south of WSP 10 and between Anneliese 1 and WSP 6.

The northern area from mapping area 1453 N to White Spur Creek Cascades contains smaller sub-basins. Several sub-basins occur and include sections ~30 m thick. These basins are still important in exploration as only a two-dimensional perspective is observed from the fence diagram. The basin geometry may expand outward (west to east) and could even contain intact Host Rock.

The Host Rock associated with the northern end is substantially greater in thickness than the southern occurrences. The two exposures are 10 and 20 m thick. This large host unit is convincing evidence that a VHMS ore deposit can be possibly hosted in the White Spur area. This area should be given high priority due to the thickness of the Host Rock in this

area.

Particularly, attention to the south of WSP 13 should be considered as the White Spur Formation is not expressed in drillhole until WSP 4. MR 1 lies to the east of the traverse between WSP 13 and WSP 4 and contains no host stratigraphy. The area between WSP 13 and WSP 4 is vast and the host rock should present. A growth fault extends through this area and may be important. To the north of WSP 13, the Host Rock wedges out over a small distance.

The 10 m Host Rock in WSP 311 could be traced south toward DCP 235 but folds evident at the surface may affect the stratigraphy at depth. The adjacent drillholes and outcrops provide no additional information. Therefore, the only way to test the Host Rock extent in this area is to drill.

The mapping area 1453 N should be mapped again to see whether or not the contact or Host Rock can be found. According to the fence diagram, there is a strong possibility that a small interval may exist as the adjacent WSP 7 and WSP 4 contain 2–4 m Host Rock.

Potentially, the Host Rock may extend continuously from WSP 13 to WSP 7, becoming thinner to the south.

The area between WSP 10 and WSP 7 is very interesting geologically compared to other areas. The Host Rock is ~5 m thick. Significant mineralisation occurs in WSP 5 as previously discussed. The dacite facies is present in the footwall and is bound by faults to the south of WSP 10 and north of WSP 7. The faults may be syn-depositional growth faults that define the sub-basins in the CVC. The dacite facies is interpreted to be intrusive into the pumiceous pyroclastic pile. Mineralisation at the contact of the CVC and the White Spur Formation host rocks occurs as replacement of primary feldspar crystals and pumice.

From all of these observed features, the following is interpreted. Hydrothermal fluids that were influenced by the emplacement of the dacite cryptodome may have formed the mineralisation. The fluids were focused along the syn-depositional growth faults, then laterally percolated through the permeable pumiceous sandstone and siltstone Host Rock replacing feldspar crystals and pumice, including the large pumice clasts. This scenario

explains the mingled siltstone in WSP 10A and the irregular and distorted laminations around the large pumice clasts and the greater concentration of sulfides close to the clasts.

Hence, the area between and surrounding WSP 10 to WSP 7 is of significance for exploration. Extensions of this mineralisation should occur away from these drillholes, with potentially significant mineralisation lying down dip or along strike between these drillholes.

The highest temperature precipitates from hydrothermal fluids are massive pyrite and pyrite-chalcopyrite mineralisation and indicate proximity to a feeder/upflow zone (Allen, 1991 unpub.). The massive pyrite in Anneliese 1 was probably derived from the North Henty Fault intersected at the bottom of the hole. Therefore, these syn-depositional growth faults are extremely important and significant in VHMS mineralisation.

The syn-depositional faults in the area have been interpreted as normal faults (Allen, 1991 unpub.; Vicary, 1998 unpub.). The only major faults observed in the area are mapped at the surface, as described above, and the fault in DCP 235. The fault that displaced the massive sulfide bearing mass-flow deposit in DCP 235 is interpreted to be a normal fault. This is evident from the additional thickness of the facies in WSP 311 but as a poorly bedded facies. This interpretation requires further study.

This example does not directly relate to the White Spur Formation and CVC contact but it illustrates that faults can remove large sections of the stratigraphy. The displacement from these faults may only be minor. Therefore, faulted-out host stratigraphy may be displaced a short distance from the original site.

Are the rhyolites related to the mineralising events? The possible effect of the dacite was discussed above with the possible influence on ore fluids. It is possible the rhyolites could have influenced the fluids in the same way but the rhyolite emplacement may be later than the mineralisation. This is possible as the rhyolite occurs higher in the stratigraphy, as in WSP 10, compared to the dacite. However, the rhyolites restricted in the lower portions of the sub-basins close to the CVC contact could have drawn hydrothermal fluids through the pumice breccia to favourable horizons.

Therefore, the areas of higher exploration potential include:

- The area between WSP 10A and WSP 7.
- The immediate area of WSP 13.
- The area between WSP 13 to WSP 4 and possibly to WSP 7.
- The immediate area surrounding WSP 311.
- The area between Anneliese 1 and WSP 6.

Further work to be considered in the White Spur area

- The sub-basins should be defined in terms of 3-dimensional shape and contained lithofacies within by searching along strike and down dip of the known basins. It is quite possible that the host sequence could be encountered.
- A more detailed volcanological analysis of the dacite facies needs to be undertaken to clarify the geometry and relationships with the extensive CVC pumice breccia.
- A detailed study on the clasts observed in the coarser intervals of the interbedded mudstone and sandstone turbidite sequence should be done. This could determine the clast origins and possibly address the origin of flow direction.
- The fossiliferous limestone clasts of the massive sulfide clast bearing mass-flow unit and the interbedded mudstone and turbidite unit could be dated, identified and used to constrain possible correlations of the White Spur Formation regionally.
- A study on the rhyolites should be carried out to determine the age of emplacement against mineralisation event and determine whether these bodies influenced mineralisation.

6.5 Summary

The White Spur stratigraphy is quite similar to the stratigraphy of the Rosebery and Hercules VHMS deposits. Correlations are possible between the Hangingwall

Volcaniclastics and the White Spur Formation. Significant mineralisation in the White Spur area includes quartz-galena veins, the massive sulfide clasts present in one of the mass-flow deposits, the massive pyrite lens in Anneliese 1 and the disseminated sulfides of WSP 5.

The updated correlations of the White Spur stratigraphy reveal several areas for potential exploration based on Host Rock presence, significant mineralisation and structural controls: the areas between WSP 10A and WSP 7, WSP 13 and WSP 4, Anneliese 1 and WSP 6, and the immediate area of WSP 13 and WSP 311.

The Exploration for the Rosebery Host Rock at White Spur along strike and down-dip in the known areas of occurrence could also prove critical to discovery of VHMS ore deposits.

Chapter 7 Summary

- The contact between the White Spur Formation and the CVC at White Spur is considered highly prospective for VHMS ore deposits.
- The CVC at White Spur includes feldspar-phyric pumice breccia, stratified pumiceous and crystal-rich sandstone and grey siltstone (Host Rock) and feldspar-phyric dacite.
- The White Spur Formation can be subdivided according composition, lithology, texture, contact relationships and depositional processes.
- There are 6 main units: include laminated pyritic black mudstone, the rhyolitic pumice-lithic breccia mass-flow deposit, the massive sulfide clast-bearing mass-flow deposit, the crystal-rich mass-flow deposit, the interbedded mudstone and sandstone turbidite unit and the quartz-feldspar-biotite-phyric rhyolite.
- Sub-basins in the CVC pumice breccia probably developed in response to syn-depositional faults. The Host Rock is preferentially preserved in these sub-basins.
- The White Spur Formation was deposited on top of the CVC and includes 3 main volcaniclastic mass-flow units that can be correlated across much of the area.
- The White Spur stratigraphy and the Rosebery-Hercules host sequence are quite similar and the White Spur Formation and Hangingwall Volcaniclastics can be correlated.
- The updated correlations of the White Spur stratigraphy reveal several areas for potential exploration, based on Host Rock presence, significant mineralisation and structural controls, such as syn-depositional growth faults and sub-basins.
- Exploration of the Host Rock along strike and down-dip in known areas of occurrence at White Spur could lead to further VHMS discoveries.

References

Allen, R.L., 1991. Structure, stratigraphy and volcanology of the Rosebery-Hercules Zn-Pb-Cu massive sulphide district, Tasmania. Report to Pasminco Exploration and Mining, Rosebery, unpublished.

Allen, R.L., 1994a. Volcanic facies analysis indicates large pyroclastic eruptions, sill complexes, synvolcanic grabens, and subtle thrusts in the Cambrian 'Central Volcanic Complex' volcanic centre, western Tasmania. Contentious issues in Tasmanian geology. Abstract Series Geological Society of Australia 39: 41-43.

Allen, R.L., 1994b. Synvolcanic subseafloor replacement model for Rosebery and other massive sulphide ores. Contentious issues in Tasmanian geology. Abstract Series Geological Society of Australia 39: 107-108

Allen, R.L., 1997. Review of RGC's Base Metal Exploration Project at White Spur, western Tasmania. Report to RGC Exploration Pty Limited, Zeehan, Tasmania, Australia, unpublished.

Allen, R.L., 1998. Review of White Spur and South Henty Exploration Projects, western Tasmania. Report to RGC Exploration Pty Limited, Zeehan, Tasmania, Australia, unpublished.

Allen & Cas, 1990. The Rosebery Controversy: distinguishing prospective submarine ignimbrite-like units from true subaerial ignimbrites in the Rosebery-Hercules ZnCuPb massive sulphide district, Tasmania. Abstract Series Geological Society of Australia 25: 31-32.

Berry, R.F., 1989. The history of movement on the Henty Fault Zone, western Tasmania: An analysis of fault striations. Australian Journal of Earth Sciences, 36: 189-205.

Brathwaite, R.L., 1970. The geology of the Rosebery ore deposits. PhD. Thesis, University of Tasmania, Hobart.

Brathwaite, R.L., 1972. The structure of the Rosebery ore deposit, Tasmania. Australasian Institute of Mining and Metallurgy, Proceedings, no. 241: 1-13.

Brathwaite, R.L., 1974. The geology and origin of the Rosebery ore deposit, Tasmania. Economic Geology, 69: 1086-1101.

Campana, B. & King, D., 1963. Palaeozoic tectonism, sedimentation and mineralization in west Tasmania. Journal of the Geological Society of Australia, 10: 1-53.

Cas, R.A.F., 1992. Submarine Volcanism: Eruption Styles, Products, and Relevance to Understanding the Host-Rock Successions to Volcanic-Hosted Massive Sulfide Deposits. Economic Geology, 87: 511-41.

Cas, R.A.F. & Wright, J.V., 1987. Volcanic Successions, Allen and Unwin, London.

Choux, C., Druitt, T. & Thomas., N, 2004. Stratification and particle segregation in flowing polydisperse suspensions, with applications to the transport and sedimentation of pyroclastic density currents. Journal of Volcanology and Geothermal Research, 138: 223-41.

Corbett, K.D., 1981. Stratigraphy and mineralization in the Mt. Read Volcanics, western Tasmania. Economic Geology and the Bulletin of the Society of Economic Geologists, 76: 209-230.

Corbett, K.D., 1992. Stratigraphic-Volcanic Setting of Massive Sulfide Deposits in the Cambrian Mount Read Volcanics, Tasmania. Economic Geology, 87: 564-586.

Corbett, K.D., 2002. Updating the geology of the Mount Read Volcanics belt. Department of Mines Tasmania, unpublished report 2002/19.

Corbett, K.D. & Lees, T.C., 1987. Stratigraphic and structural relationships and evidence for the Cambrian deformation at the western margin of the Mt Read Volcanics, Tasmania. Australian Journal of Earth Sciences, 34: 45-67.

Corbett, K.D., Solomon, M., McClenaghan, M.P., Carswell, J.T., Green, G.R., Iliff, G.,

Howarth, J.W., McArthur, G .J. & Wallace, D.B., 1989. Cambrian Mt Read Volcanics and associated mineral deposits. Geology and mineral resources of Tasmania, Special Publication, Geological Society of Australia, 15: 84-153.

Crawford, A.J. & Berry, R.F., 1992. Tectonic implications of Late Proterozoic-Early Palaeozoic igneous rock associations in western Tasmania. Tectonophysics, 214: 37-56.

Crawford, A.J., Corbett, K.D. & Everard, J.L., 1992. Geochemistry of the Cambrian Volcanic-Hosted Massive Sulfide-Rich Mount Read Volcanics, Tasmania, and Some Tectonic Implications. Economic Geology, 87: 597-619.

Dugdale, J., 1992. Lithostratigraphy of the White Spur area, western Tasmania, Hons Thesis, University of Tasmania, Hobart.

Gifkins, C.C., 2001. Submarine volcanism and alteration in the Cambrian, northern Central Volcanic Complex, western Tasmania. Ph.D. Thesis, University of Tasmania, Hobart.

Gifkins, C.C., McPhie. J. & Allen, R.L., 2002. Pumiceous rhyolitic peperite in ancient submarine volcanic successions. Journal of Volcanology and Geothermal Research, 114: 181-203.

Gifkins, C.C., Herrmann. W & Large, R.R., 2005a. Altered Volcanic Textures: A Guide to Description and Interpretation. CODES, University of Tasmania, Hobart.

Gifkins, C.C., Allen, R.L. & McPhie, J., 2005b. Apparent welding textures in altered pumice-rich rocks. Journal of Volcanology and Geothermal Research, 142: 29-47.

Green, G.R., Solomon, M. & Walshe, J., L., 1981. The Formation of the Volcanic-Hosted Massive Sulfide Ore Deposit at Rosebery, Tasmania. Economic Geology, 76: 304-338.

Hunns, S.R. & McPhie. J., 1999. Pumiceous peperite in a submarine volcanic succession at

Mount Chalmers, Queensland, Australia. Journal of Volcanology and Geothermal Research, 88: 239-254.

Kano, K., 1996. A Miocene coarse volcaniclastic mass-flow deposit in the Shimane Peninsula, SW Japan: product of a deep submarine eruption? Bulletin of Volcanology, 58: 131-43.

Large, R.R., Allen, R., L., Blake, M., D. & Herrmann, W., 2001. Hydrothermal Alteration and Volatile Element Haloes for the Rosebery K Lens Volcanic-Hosted Massive Sulfide Deposit, Western Tasmania. Economic Geology, 96: 1055-1072.

Large, R.R., 1992. Australian Volcanic-Hosted Massive Sulfide Deposits: Features, Styles, and Genetic Models. Economic Geology, 87: 471-510.

Lash, G.G. & Blood, D., 2004. Geochemical and textural evidence for early (shallow) diagenetic growth of stratigraphically confined carbonate concretions, Upper Devonian Rhinestreet black shale, western New York. Chemical Geology, 206: 407-424.

Lees, T.C., 1987. Geology and Mineralization of the Rosebery - Hercules Area, Tasmania. MSc Thesis, University of Tasmania, Hobart.

Lowe, D.R., 1982. Sediment gravity flows: II. Depositional models with special reference to the deposits of high density turbidity currents. Journal of Sedimentary Petrology, 52: 279-297.

McPhie, J. & Allen, R.L., 1992. Facies Architecture of Mineralized Submarine Volcanic Sequences: Cambrian Mount Read Volcanics, Western Tasmania. Economic Geology, 87: 587-596.

McPhie, J. & Allen, R.L., 2003. Submarine, Silicic, Syn-Eruptive Pyroclastic Units in the Mount Read Volcanics, Western Tasmania: Influence of Vent Setting and Proximity on Lithofacies Characteristics. AGU Geophysical Monograph, 140: 245-258.

McPhie, J., Doyle, M. & Allen, A.L., 1993. Volcanic Textures: A Guide to the Interpretation of Textures in Volcanic Rocks. CODES, University of Tasmania, Hobart.

Munker, C. & Crawford, A.J., 2000. Cambrian arc evolution along the SE Gondwana active margin: A synthesis from Tasmania-New Zealand-Australia-Antarctica correlations. Tectonics, 19: 415-432.

Nunn, T., 1995. The sedimentology, volcanology, and structure of the Lower Dundas Group, Hall Rivulet Canal, western Tasmania. Hons Thesis, University of Tasmania, Hobart.

Pickering, K.T., Hiscott, R.N. & Hein, F.J., 1989. Deep Marine Environments: Clastic Sedimentation and Tectonics. Unwin Hyman Limited.

Piper. D.Z. & Perkins R.B., 2004. A modern vs. Permian black shale-the hydrography, primary productivity, and water-column chemistry of deposition. Chemical Geology, 206: 177-197.

Reading, H.G., 1986. Sedimentary Environments and Facies. Blackwell Scientific Publication.

Skilling, I.P., White, J.D.L & McPhie, J, 2002. Peperite; a review of magma-sediment mingling. Journal of Volcanology and Geothermal Research, 114: 1-17.

Solomon, M., Tornos, F., Large, R.R., Badham, J.N.P., Both, R.A. & Zaw, K., 2004. Zn-Pb-Cu volcanic-hosted massive sulfide deposits: criteria for distinguishing brine pool-type from black smoker-type sulfide deposition, Ore Geology Reviews, 25: 259-283.

Vicary, M., 1998. Tasmanian Base Metals Project EL 5/96. White Spur. AGC Exploration Annual Report, unpublished.

Walker, R.G., 1984. Facies Models. Second Edition. Geological Association of Canada

Publications.

White, M.J. & McPhie, J., 1996. Stratigraphy and palaeovolcanology of the Cambrian Tyndall Group, Mt Read Volcanics, western Tasmania. Australian Journal of Earth Sciences, 43: 147-159.

White, M.J. & McPhie, J., 1997. A submarine welded ignimbrite-crystal-rich sandstone facies association in the Cambrian Tyndall Group, western Tasmania, Australia. Journal of Volcanology and Geothermal Research, 76: 277-295.

Zaw, K., Huston, D.L. & Large, R.R., 1999. A Chemical Model for the Devonian Remobilization Process in the Cambrian Volcanic-Hosted Massive Sulfide Rosebery Deposit, Western Tasmania. Economic Geology, 94: 529-546.

Zaw, K. & Large, R.R., 1992. The Precious Metal-Rich South Hercules Mineralization, Western Tasmania: A Possible Subsea-Floor Replacement Volcanic-Hosted Massive Sulfide Deposit. Economic Geology, 87: 931-952.

Appendix